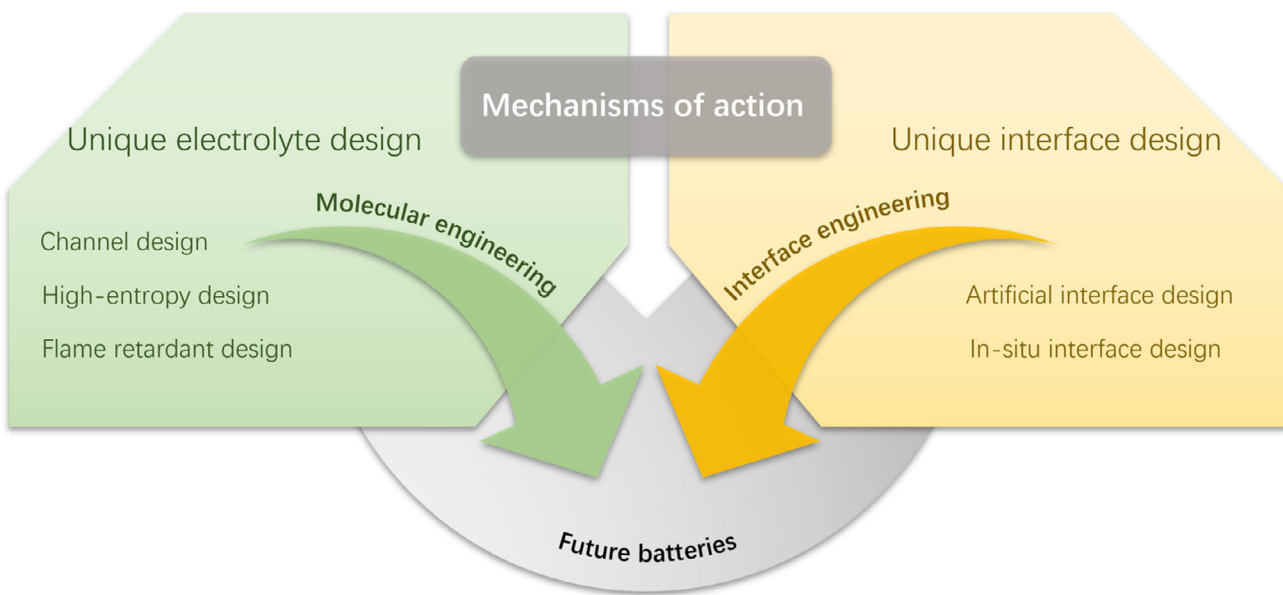


Unique Design Strategies for High-Performance Solid-State Polymer Batteries

Wenhai Xu, Libo Li,* Hang Yang, Suo Li, and Zhixuan Wang



Solid polymer electrolytes (SPEs) are considered a key enabler for high-safety and high-energy-density solid-state lithium-metal batteries. However, challenges such as low ionic conductivity, poor interfacial compatibility, and limited thermal stability continue to hinder their practical application. This review explores the interaction mechanisms in SPEs in detail from four aspects—Lewis acid-base theory, anion vacancies, hydrogen-bond networks, and phase-separated structures—and introduces three functionalized

design strategies: channel design, high-entropy design, and flame-retardant design. We also comprehensively discuss the latest advancements and development potential in artificial interface design and in situ interface design. This article outlines strategies to overcome existing bottlenecks and emphasizes the importance of functional design. By modulating these microinteractions and optimizing design strategies, it will help accelerate the commercialization of high-safety, high-energy-density solid-state batteries.

1. Introduction

As the global energy landscape evolves and renewable energy technologies advance at a rapid pace, efficient and safe energy storage technologies have become key drivers of sustainable development in modern society.^[1–12] Lithium-ion batteries (LIBs), which are currently the predominant energy storage solution, have found extensive use in portable electronics, electric vehicles, and smart grid systems. However, conventional liquid electrolyte systems present safety risks such as flammability and leakage, and their energy density is approaching the theoretical limit, making it difficult to meet the dual demands of high energy density and high safety for next-generation energy storage devices.^[13–19] Against this backdrop, solid-state electrolytes (SSEs) eliminate the use of solvents and have attracted increasing attention due to their potential for high energy density.^[20–26] SSEs exhibit high mechanical properties, which help resist the growth of lithium dendrites and short circuits. Still, their low Li⁺ conductivity and poor interface compatibility with solid-state electrodes severely hinder the development of solid-state electrolytes.^[27–35]

Compared to inorganic ceramic electrolytes, SPEs offer better flexibility and interface contact properties, which can effectively alleviate the issue of high interfacial impedance during charge and discharge processes. At the same time, the preparation process of SPEs is relatively simple, and they are easy to scale up for mass production, making solid-state battery commercialization a promising prospect.^[36–42] However, despite the many potentials of SPEs, their practical application still faces a series of technical challenges. First, their room-temperature ionic conductivity is typically low, making it difficult to meet the demands of high-power batteries. Second, the narrow electrochemical stability window of SPEs restricts their compatibility with high-voltage cathodes, thereby hindering the potential to increase energy density. Furthermore, the stability of the electrode/electrolyte interface is also a critical factor restricting the performance of SPEs, as interfacial side reactions and lithium dendrite growth can significantly reduce the cycling life and safety of batteries.^[43–51] Therefore, deepening the understanding of ion transport in SPEs and optimizing

their properties through functional design are essential to enhancing battery safety and performance.

The performance optimization of SPEs involves multiple dimensions, such as ionic conductivity, mechanical strength, interface stability, and safety. It is essentially a comprehensive manifestation of the complex internal interaction mechanisms within the materials.^[52–54] At the molecular scale, the performance of SPEs is closely linked to their microstructure, intermolecular interactions, and ion transport behavior. Recent advances in molecular design, structural engineering, and filler incorporation have significantly enhanced their cycling performance. For example, by incorporating functional fillers (such as alumina and silica) or designing polymer matrices with specific functional groups (such as sulfonic acid groups), efficient ion transport channels have been successfully constructed, significantly enhancing the ionic conductivity of SPEs.^[55–60] Nevertheless, practical applications of SPEs still face some key issues. For instance, how to balance ionic conductivity with mechanical performance, how to optimize the electrode/electrolyte interface stability to suppress lithium dendrite growth, and how to improve the adaptability of SPEs under extreme conditions.^[61–64] Solving these problems requires deeper exploration from multiple perspectives, including molecular design and interface regulation.

This review aims to systematically elaborate on the key mechanisms of action in SPEs and their functional design strategies (Figure 1). First, it delves into the ion transport mechanisms and structure-performance relationships in SPEs from four aspects: Lewis acid-base theory, anion vacancies, hydrogen-bond networks, and phase-separated structures. Next, it highlights the latest advancements in advanced functional strategies, such as channel design, high-entropy design, and flame-retardant design, in optimizing the performance of SPEs. Then, addressing the electrode/electrolyte interface issue, the review discusses in detail the strategies of artificial interface design and in situ interface design and their impact on battery performance. Finally, we provide a thorough summary of the covered topics and offer forward-looking perspectives and insights. We hope this review will inspire more researchers to engage in the development of novel SPEs, thereby driving further advancements in the field of solid-state batteries and accelerating their commercialization.

2. Mechanisms of Action in Polymer Electrolytes

As a functional material combining the processability of polymer materials with ionic conductivity, polymer electrolytes have

W. Xu, L. Li, H. Yang, S. Li, Z. Wang
School of Materials Science and Chemical Engineering
Harbin University of Science and Technology
Harbin 150080, China
E-mail: lilib@hrbust.edu.cn

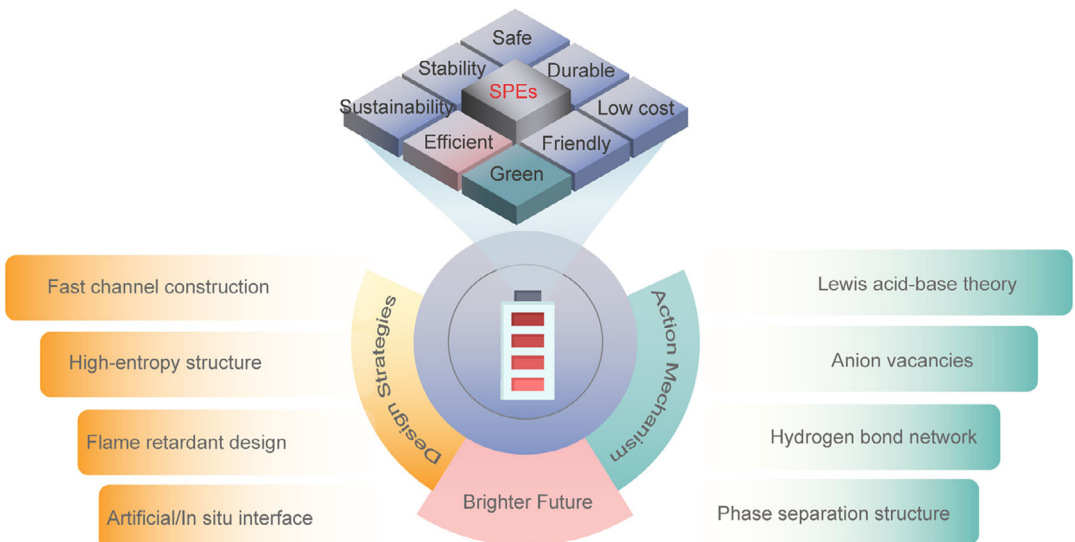


Figure 1. Overview diagram of the main content of this article.

shown enormous application potential in fields such as solid-state batteries, fuel cells, and supercapacitors. Their ionic conductivity is closely related to the complex internal interactions of the materials, and these mechanisms collectively determine the microstructure of the electrolyte and ion transport behavior. This chapter systematically elaborates on the key mechanisms in polymer electrolytes from four aspects: Lewis acid-base theory, anion vacancies, hydrogen bonding, and phase separation with microstructure.

2.1. Lewis Acid-Base Theory

In the field of energy storage, Lewis acid-base interactions play a decisive role in the core electrochemical performance indicators—activity, selectivity (efficiency), and stability. These indicators are key scientific issues faced by various battery systems and directly determine their practical application performance. By regulating Lewis acid-base interactions, the microenvironment of the electrolyte can be effectively optimized, such as altering the solvation structure, which accelerates ion diffusion dynamics and enhances charge transfer efficiency, ultimately improving the battery's energy storage capacity.^[65–67] Studies have shown that Lewis acid/base additives can regulate the electron transfer pathway and significantly reduce the energy barrier for electrophilic/nucleophilic intermediate conversion in active materials. This

mechanism provides new insights into improving the specific capacity and rate performance of batteries. From a selectivity perspective, increasing the cation migration number not only alleviates concentration polarization but also effectively suppresses side reactions, which is crucial for improving the energy efficiency and high-speed charge/discharge performance of batteries. Functional donor–acceptor molecules designed based on Lewis acid-base theory provide theoretical guidance for ion selectivity regulation in electrolyte systems.^[68–70] In terms of stability, the coordination effect of the Lewis acid/base centers can precisely regulate the electronic structure of the electrolyte by widening the HOMO-LUMO energy gap, thereby enlarging the electrochemical stability window.^[71] Furthermore, this interaction can strengthen the structural stability of electrode materials and improve the interface adsorption ability of active substances, effectively suppressing material dissolution and significantly extending the cycle life of the battery.

In SPEs, the practical application of Lewis acid-base theory is mainly reflected in two aspects: functional modification of the polymer matrix and the introduction of inorganic fillers with specific surface chemical properties. Among them, this theory shows unique advantages in optimizing cation transport behavior, particularly playing a key role in regulating ion selectivity and conductivity. Typically, Lewis acid-base interactions promote ion conduction in SPEs through three mechanisms: controlling ion dissociation degree, optimizing ion transport pathways, and



Wenhao Xu received his bachelor's degree from the Harbin University of Science and Technology in 2018. He is currently pursuing his master's degree at the School of Materials Science and Chemical Engineering, Harbin University of Science and Technology, under the supervision of Professor Libo Li. His research mainly focuses on the performance of lithium-ion batteries, particularly the design, fabrication, and underlying mechanisms of solid-state polymer lithium batteries.



Libo Li received her Ph.D. in Applied Chemistry from Harbin Institute of Technology in 2006. She is currently a professor at the School of Materials Science and Chemical Engineering, Harbin University of Science and Technology. Over the years, she has conducted extensive research in electrochemical theory and applications, including key materials and devices related to solid-state lithium batteries, lithium-ion batteries, and lithium-sulfur batteries.

altering the movement characteristics of polymer chain segments. Furthermore, this interaction also significantly impacts the physicochemical properties of SPEs, including changing the glass transition temperature of the material, enhancing high-voltage tolerance, and improving mechanical properties.

Montmorillonite (MMT) rich in Lewis acid centers is commonly used as a filler in SPEs to enhance overall performance. Zhao et al.^[72] successfully constructed an efficient 3D lithium-ion transport network by combining organically modified MMT (OMMT) with various polymers (Figure 2a,b). The Lewis acid centers of OMMT significantly promoted the dissociation of lithium salts, enhancing the migration rate and conductivity of lithium ions. OMMT is characterized by aluminum–oxygen octahedra intercalated between silicon–oxygen tetrahedra. This structure provides a rich negatively charged surface that can adsorb cations and promote the dissociation of lithium salts through its Lewis acid centers. The addition of OMMT not only reduced the crystallinity of the polymer but also formed a porous structure, providing good lithium-ion migration channels. Specifically, the Lewis acid centers of OMMT fixed the TFSI⁻ anion, thereby improving the lithium-ion migration number, reaching as high as 0.54. Similarly, Chang et al.^[73] proposed a new strategy for modifying PVDF-HFP-based polymer solid-state electrolytes using inorganic fillers with frustrated Lewis pairs (FLPs) and achieved long-lasting reversible cycling of lithium metal batteries (Figure 2c). The FLPs designed in nickel borate provide dual functional sites, where the Lewis acid site interacts with the anion in the lithium salt to promote its dissociation, while the Lewis base site interacts with lithium

ions and acts as an active site to assist lithium-ion migration. The resulting SPE-NiBO-150 polymer solid-state electrolyte exhibited a high ionic conductivity of $4.92 \times 10^{-4} \text{ S cm}^{-1}$, a high Li⁺ transfer number of 0.74, and excellent interface compatibility with lithium anodes and LiFePO₄ cathodes at room temperature. The assembled lithium symmetric cells demonstrated ultralong cycling stability (with a lifetime exceeding 10 000 h at current densities of 0.2 and 0.5 mA cm⁻²), and the assembled full battery also exhibited excellent performance (maintaining 86% of the capacity after 300 cycles at 0.5 C). An et al.^[74] demonstrated a Lewis acid-coordinated PEO-based electrolyte for achieving high-energy 4.8 V-class batteries (Figure 2d,e). By introducing Mg²⁺ and Al³⁺ with strong electron-withdrawing abilities, the highly electronegative EO chains were captured, weakening their ability to dissolve high-valent nickel under high voltage. This effect reduced the strong reactivity between EO groups and LiNi_{0.83}Co_{0.12}Mn_{0.05}O₂ cathodes at 4.8 V, significantly improving interface compatibility. The full batteries assembled based on this design achieved 300 cycles at 4.8 V high voltage, with an energy density exceeding 586 Wh kg⁻¹.

Overall, the Lewis acid-base theory provides important theoretical guidance for the design and optimization of SPEs. By functionalizing the polymer matrix or introducing inorganic fillers, the Lewis acid-base interactions can significantly enhance the ionic conductivity, lithium-ion transfer number, and interface stability of SPEs. Specifically, the Lewis acid centers promote lithium salt dissociation, fix anions, and optimize ion transport paths, effectively improving ion transport dynamics. At the same time, Lewis

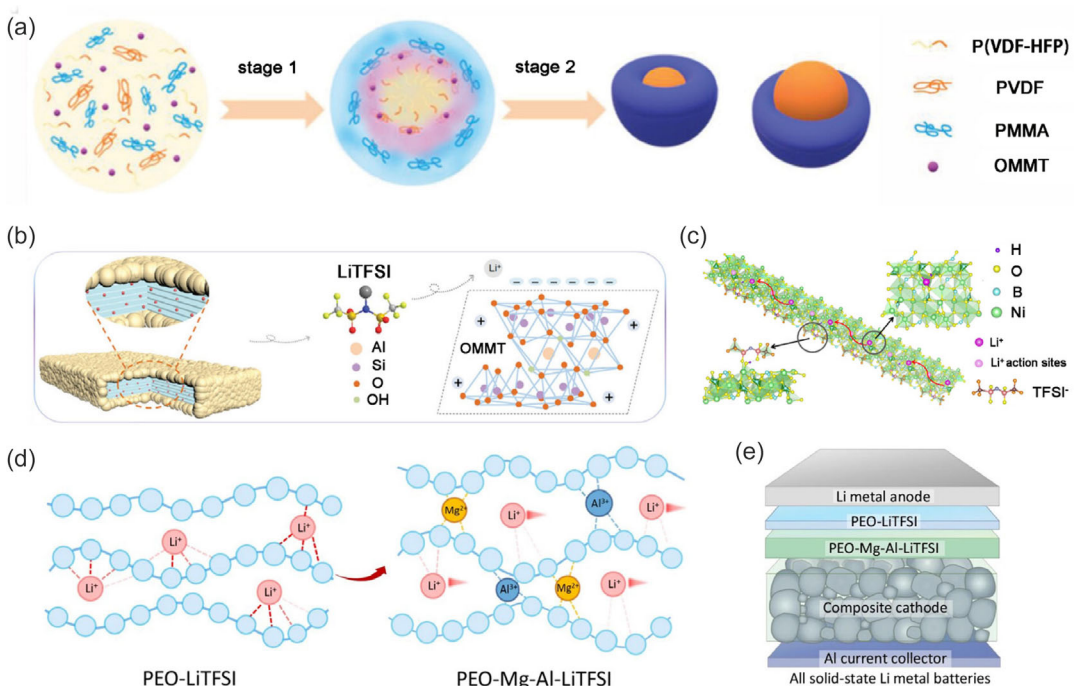


Figure 2. a) The schematic diagram depicts the process through which a porous structure is formed within PE. b) The Schematic diagram demonstrates how OMMT facilitates lithium-ion migration. Reproduced with permission.^[72] Copyright 2023, Wiley-VCH. c) A schematic diagram depicts the dissociation of lithium salts and the transport of Li⁺ through nickel borate, which features dual-active sites. Reproduced with permission.^[73] Copyright 2024, Elsevier. d) A schematic illustrating the role of Lewis-acid additives. e) A schematic depicting the structure of PEO-Mg-Al-LiTFSI batteries. Reproduced with permission.^[74] Copyright 2024, Springer Nature.

acid–base interactions enhance the mechanical properties and electrochemical stability of the electrolyte by regulating polymer chain dynamics, reducing crystallinity, and improving interface compatibility. These characteristics make SPEs designed based on the Lewis acid-base theory and show great application potential in lithium metal batteries with high voltage and long cycling life.

2.2. Anion Vacancies

The formation and distribution of anion vacancies in polymer electrolytes significantly impact ion transport behavior. Anion vacancies are not only key to ion migration but also affect the electrochemical performance of the electrolyte by regulating the local electric field and ion-polymer interactions. The presence of anion vacancies can effectively anchor anions, promote lithium salt dissociation, and thereby enhance the lithium-ion transfer number. Moreover, the distribution characteristics of anion vacancies are closely related to the electrolyte's microstructure, and their order and density directly influence the continuity and efficiency of ion transport paths.^[75,76] By rationally designing the quantity and spatial distribution of anion vacancies, the ion selectivity of the electrolyte can be optimized, reducing concentration polarization and suppressing side reactions.^[77,78] In recent years, researchers have successfully achieved precise control over anion vacancies through the introduction of functional fillers, regulation of polymer chain segment movement, and optimization

of preparation processes, providing new insights for the development of high-performance polymer electrolytes.

Although positively charged anion vacancies (oxygen or sulfur vacancies) in inorganic materials can promote lithium salt dissociation and enhance lithium-ion conductivity, most inorganic fillers exhibit weak interactions with polymers, leading to poor mechanical properties of composite electrolytes and even phase separation between the filler and polymer, thus limiting their performance enhancement. Therefore, designing inorganic fillers rich in vacancies that are compatible with polymers is essential. Liu et al.^[79] demonstrated that the anion vacancies in the fillers can anchor the anions of lithium salts, significantly increasing the lithium-ion migration number in the electrolyte. Based on this, they prepared flower-like tin disulfide (SnS_2) composites with abundant sulfur vacancies under the regulation of functionalized carbon dots, which were used to construct composite polymer solid-state electrolytes (Figure 3a). The synthesized SnS_2 /carbon dot composite materials exhibited a 3D flower-like structure, with a large specific surface area that effectively increased the contact area with the polymer. When combined with PEO-based solid-state electrolytes, the ion conductivity and mechanical properties were significantly improved. The sulfur vacancies effectively anchored the anions, resulting in a lithium-ion migration number of 0.786 for the composite electrolyte. Density functional theory (DFT) calculations showed that at the interface rich in sulfur vacancies, the lithium-ion diffusion barrier was lowered, optimizing the internal microenvironment of the electrolyte and creating

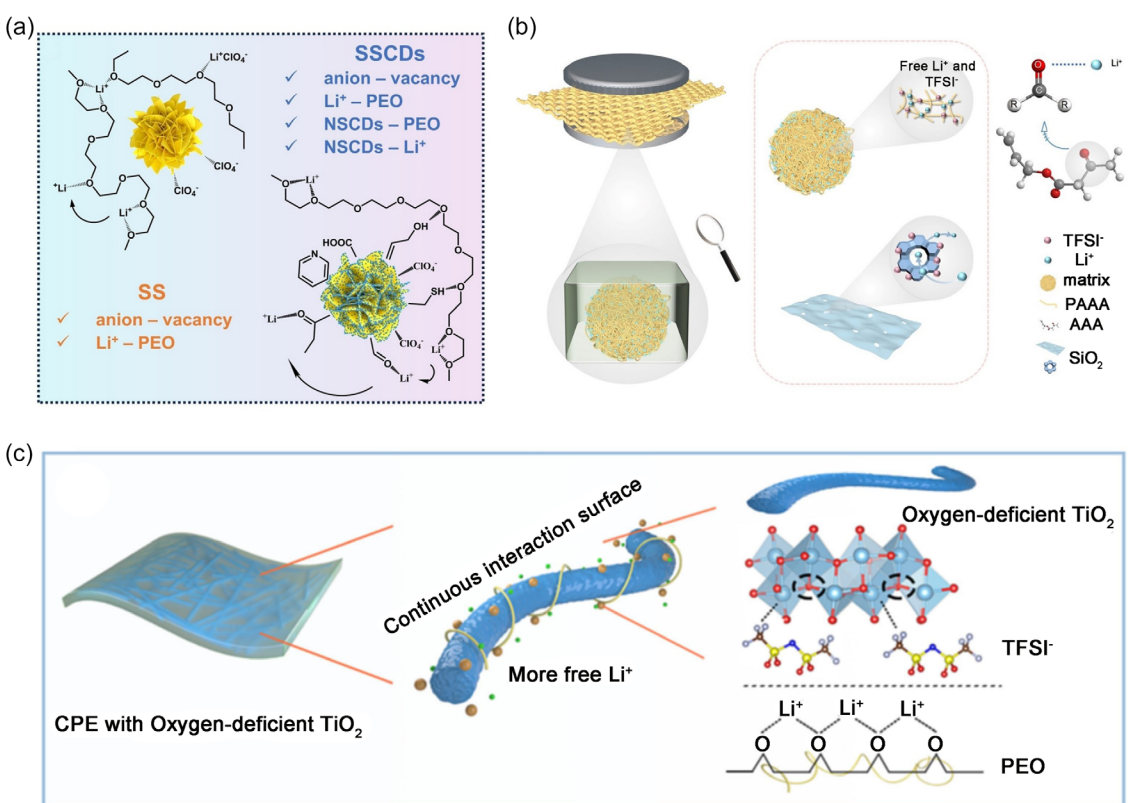


Figure 3. a) A schematic illustrating the interactions within SS and SSCDs. Reproduced with permission.^[79] Copyright 2024, Wiley-VCH. b) A schematic diagram of LPAS SPE. Reproduced with permission.^[80] Copyright 2024, Wiley-VCH. c) Schematic diagrams depicting the surface interactions of oxygen-deficient TiO_2 in CPEs. Reproduced with permission.^[81] Copyright 2023, Elsevier.

fast diffusion channels for lithium ions. Furthermore, the *in situ* generated Li₂S/Li₃N interface layer during cycling accelerated lithium-ion diffusion at the interface and induced uniform lithium deposition, effectively suppressing dendrite growth. Therefore, the lithium symmetric cells assembled with this composite electrolyte exhibited stable cycling for over 1300 h. The full battery constructed using this composite electrolyte demonstrated excellent electrochemical stability and rate performance. This work provides a new strategy for the design of composite electrolytes by modifying inorganic fillers with carbon dots. Similarly, Zhao et al.^[80] introduced layered inorganic SiO₂ nanosheets rich in oxygen vacancies into SPEs to anchor TFSI⁻ anions and promote rapid Li⁺ migration (Figure 3b). Through molecular dynamics simulations and DFT calculations, they confirmed the strong adsorption interaction between SiO₂ and TFSI⁻, further enhancing Li⁺ conduction. Additionally, the high specific surface area and 2D layered structure of SiO₂ nanosheets effectively suppressed lithium dendrite growth, improving battery safety. This innovative method enabled SPEs to exhibit excellent performance, with an ion conductivity of 3.82×10^{-4} S cm⁻¹ at room temperature and a lithium-ion migration number of 0.66. Luo et al.^[81] proposed a new strategy to enhance SPE performance through morphological and defect engineering. Their team introduced 1D TiO₂ nanorods rich in oxygen vacancies into PEO-based SPEs (Figure 3c). This approach not only increased the amorphous phase of the PEO matrix but also promoted stronger anion adsorption, improving the uniformity and stability of the electrolyte-electrode interface. The oxygen vacancies on the surface of TiO₂ nanorods played a key role in dissociating LiTFSI, increasing the concentration of free Li⁺ and thereby improving overall ion conductivity. Specifically, the lithium symmetric cells achieved ultralong cycle life for over 1000 h at a current density of 0.2 mA cm⁻². Moreover, the full metal battery with a LiFePO₄ cathode demonstrated perfect cycle performance (with a capacity of 162.4 mAh g⁻¹ after 200 cycles at 0.33 C) and rate performance (with a capacity of 132 mAh g⁻¹ at 2 C).

Overall, the introduction of anion vacancies provides a new dimension for the optimization of polymer electrolyte performance. Through the design and regulation of functional fillers, precise construction of anion vacancies can be achieved, significantly enhancing the ion transport efficiency and interface stability of the electrolyte. The constructed anion vacancies not only improve the lithium-ion migration number by anchoring the anions but also optimize the transport path by lowering the ion diffusion barrier. Additionally, the presence of anion vacancies effectively suppresses the growth of lithium dendrites, enhancing the battery's safety and cycling stability. Therefore, the rational design and regulation of anion vacancies is one of the key strategies for overcoming the ion transport bottleneck in polymer electrolytes.

2.3. Hydrogen Bond

Hydrogen bonds, as key intermolecular interactions, play a vital role in polymer electrolytes by acting as physical crosslinking points to enhance mechanical properties and by regulating

ion transport pathways and solvation structures to influence ionic conduction. The formation of hydrogen bonds depends on electrostatic interactions between donors (such as hydroxyl and amino groups) and acceptors (such as oxygen and nitrogen atoms), and their strength and directionality have a profound impact on the structure and performance of the electrolyte.^[82–85] The presence of hydrogen bond networks can effectively reduce the energy barrier for ion migration, promote ion hopping conduction, and stabilize the electrode-electrolyte interface to suppress side reactions. In recent years, researchers have successfully achieved precise regulation of hydrogen bond networks by designing functional polymers with specific hydrogen bond donor/acceptor groups, providing new ideas for developing high-performance polymer electrolytes.^[86–88] This section will systematically explore the mechanism of hydrogen bond interactions in polymer electrolytes, regulation strategies, and their impact on ion transport behavior, offering a theoretical basis and practical guidance for further optimization of electrolyte performance.

Polyurethane (PU)-based electrolytes have garnered growing interest owing to their remarkable flexibility in operation, superior mechanical strength, exceptional thermal stability, and stable electrochemical performance. By altering terminal monomers (such as –NCO, –NH₂, and OH), various types of PUs can be obtained, enabling flexible structural design. Among them, hydrogen bonds formed by –NH provide PU-based electrolytes with good self-healing and adhesion properties, owing to their excellent interfacial compatibility and safety performance.^[89,90] Recently, Ye et al.^[91] introduced a novel self-healing PU (PNPU) and combined it with commercial PVDF-HFP to successfully prepare a composite solid polymer electrolyte (PNPU-PVDF-HFP SPEs) with significantly improved mechanical-electrochemical coupling performance. The team validated the existence of multiple hydrogen bond modes in PNPU through theoretical calculations and characterization, which not only endowed PNPU with superior mechanical properties but also promoted weak interactions between it and the PVDF-HFP matrix, forming a compact membrane structure (Figure 4a). More importantly, PNPU provided additional migration pathways for lithium ions, significantly enhancing the ion conductivity of PNPU-PVDF-HFP SPEs to 4.13×10^{-4} S cm⁻¹, far exceeding the performance of PVDF-HFP alone. Specifically, the ether groups in PNPU provided active sites for lithium-ion migration, while the dense hydrogen bond network formed by isocyanate and ether groups enhanced the overall mechanical strength and thermal stability of the system. This shows that the hydrogen bonds formed between the matrixes are crucial for maintaining the stability of the hybrid polymer framework. Wang et al.^[86] emphasized the role of local intermolecular interactions—particularly hydrogen bonds—as key factors in improving antioxidant performance and lithium ion migration mechanisms. Both experimental and theoretical calculations confirmed the hydrogen bond network formed between polymer chains and TFSI⁻ anions (Figure 4b), which not only led to longer bond lengths and lower bond energies but also promoted red-shift phenomena in the characteristic peaks, thereby enhancing the overall performance of the polymer electrolyte. It is noteworthy that for monomers containing hydrogen bond donors (such as amino, hydroxyl, and carboxyl groups)

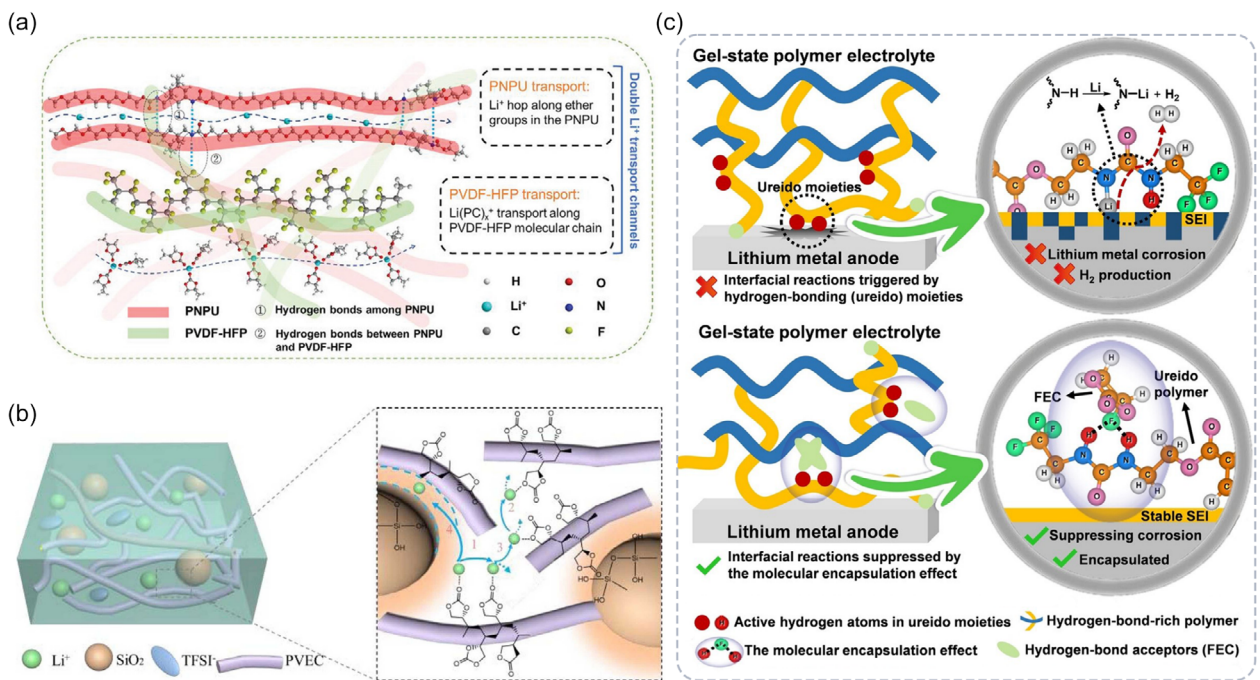


Figure 4. a) Supramolecular interactions and Li⁺ transport channels in PNPU-PVDF-HFP SPEs. Reproduced with permission.^[91] Copyright 2023, Wiley-VCH. b) A schematic illustrating the Li⁺ transport pathways in the CSE. Reproduced with permission.^[86] Copyright 2022, Elsevier. c) A schematic diagram of the interfacial reactions involving hydrogen-bond-rich gel-state polymer electrolytes and LMAs. Reproduced with permission.^[92] Copyright 2024, Wiley-VCH.

after polymerization, their active hydrogen atoms can undergo substitution reactions with the lithium anode, leading to polymer degradation, interface deterioration, and hydrogen gas release. Xu et al.^[92] explored the important role of the molecular encapsulation effect in enhancing the chemical stability of hydrogen-bond-rich SPEs. By introducing hydrogen bond acceptors into SPEs, the chemical reactivity of active hydrogen atoms can be effectively regulated, thereby reducing interface corrosion with the lithium metal anode (Figure 4c). The results showed that the added hydrogen bond acceptors, through intermolecular hydrogen bond interactions, could “wrap” active hydrogen atoms, reducing their contact with the lithium metal surface and significantly enhancing the chemical stability of the polymer structure and interface. After applying this strategy, the 1.1 Ah capacity LiNi_{0.8}Co_{0.1}Mn_{0.1}O₂/Li pouch cell still retained 96.3% of its initial capacity after 100 cycles, demonstrating that this method provides a feasible path for constructing high-stability lithium metal batteries.

Therefore, the role of hydrogen bonds in polymer electrolytes is not limited to enhancing mechanical performance and interface stability; their regulatory role in ion transport dynamics is also receiving increasing attention. However, the strong directionality and intensity of hydrogen bonds may also increase the rigidity of polymer chains, thereby limiting the ion migration rate. Future research should further explore the synergistic effects of hydrogen bonds with other mechanisms (such as anion vacancies and phase separation) to achieve a balanced optimization of mechanical performance and ion conductivity. Through molecular design and interface engineering, hydrogen bond regulation strategies are expected to provide new breakthroughs for the development of high-performance polymer electrolytes.

2.4. Phase Separation and Microdomain Structure

In SPEs, constructing phase-separated microstructures often allows for effective control over the material's properties. The phase separation phenomenon is typically driven by the thermodynamic incompatibility between polymer segments and salts, plasticizers, or other functional components, leading to component segregation and the formation of multiphase structures at the microscopic scale.^[93] The morphology of these microstructures (e.g., island structure, double continuous phase, or layered structure) has a certain impact on the ion transport path, interface contact state, and mechanical properties of the electrolyte. Typically, by rationally designing phase-separated SPEs, continuous ion transport channels can be constructed, significantly improving ion conductivity, while the synergistic effect of hard and soft phases enhances the material's mechanical strength and toughness.^[94–96]

Recently, polymerization-induced phase separation (PIPS) designed plastic crystal-embedded elastomer electrolytes (PCE) have emerged as promising SPEs for achieving high ionic conductivity and excellent mechanical elasticity. The PIPS method involves capturing ion-conducting domains (e.g., plastic crystals) within the in situ grown cross-linked polymer matrix, thereby forming a bicontinuous structure consisting of ion-conducting phases and mechanically robust elastic phases. Han et al.^[97] proposed a phase-separated SPE system that includes a fluorine-containing elastomer phase, assembled via in situ polymerization of trifluoroethyl acrylate (TFEA) with plastic crystals (Figure 5a,b). In contrast to the ethyl acrylate-based solid polymer electrolyte (E-SPE), which exhibits no phase separation and lacks fluorine chemistry, the TFEA-based SPE (T-SPE) demonstrates

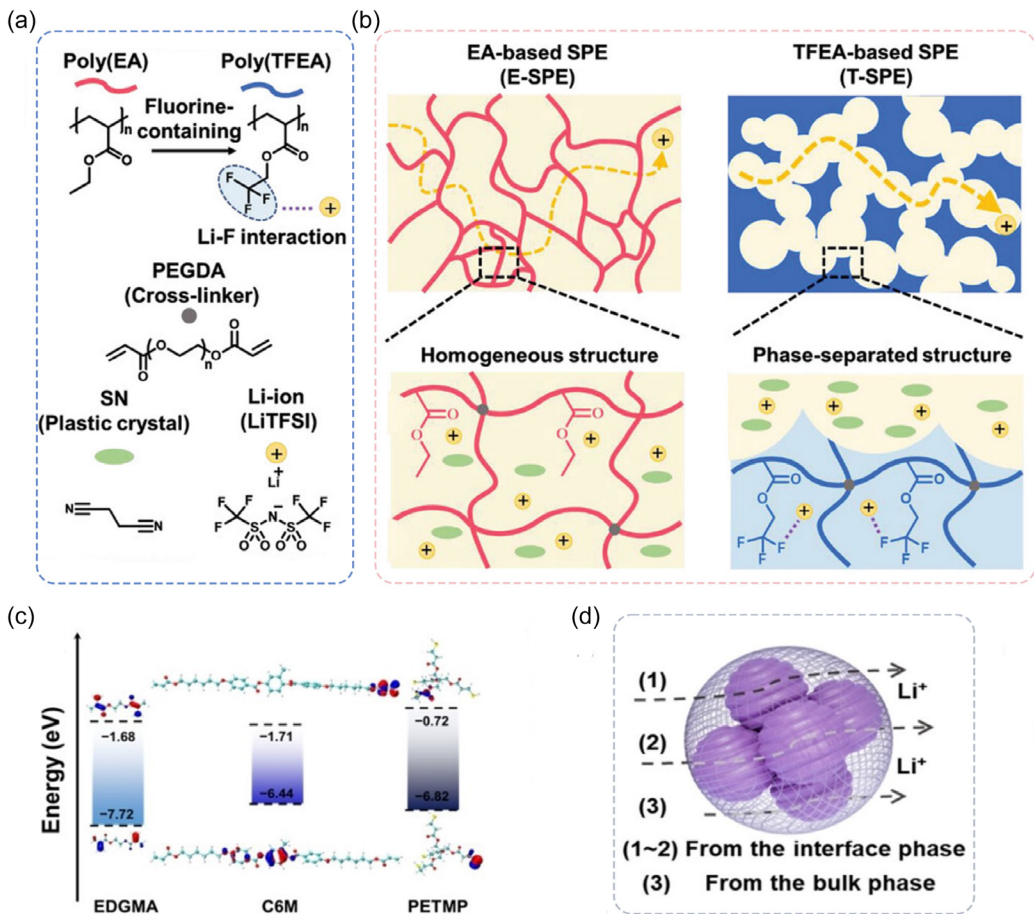


Figure 5. a) The materials employed in the fabrication of E-SPE and T-SPE. b) Diagrams showing the morphologies of E-SPE and T-SPE. Reproduced with permission.^[97] Copyright 2024, Wiley-VCH. c) The HOMO and LUMO energy levels of EDGMA, C6M, and PETMP. d) A schematic depicting nanoparticle and their surface functional groups in RMSPE. Reproduced with permission.^[98] Copyright 2024, Wiley-VCH.

notable advancements in both mechanical and electrochemical properties, along with improved interfacial stability. Unlike the uniform structure of E-SPE, T-SPE exhibits a bicontinuous morphology, where ion-conducting plastic crystals are interconnected, due to the immiscibility between in situ polymerized TFEA and plastic crystal domains. Therefore, even under extreme operating conditions with a low N/P ratio (<0.5), thin Li foil (5 µm), and high-loading LiNi_{0.83}Mn_{0.06}Co_{0.11}O₂ cathodes, solid-state LMBs based on T-SPE achieve an energy density of up to 538 Wh kg⁻¹ and maintain a high-power output of 804 W kg⁻¹. Ma et al.^[98] proposed a design concept for multicomponent ion-conducting electrolytes based on a refined multistructural polymer electrolyte (RMSPE) framework. This framework is constructed using PIPS technology and optimized by rationally combining lithium-affinity components with rigid/flexible chain units that exhibit significant hydrophobic/hydrophilic contrast (Figure 5c,d). By coating a robust polymer network, this all-organic design forms a uniform micronanoporous structure, providing a new framework for rapid ion transport, and performing excellently in both its soft interface and bulk phase. As a result, the RMSPE achieves a high ionic conductivity of 1.91×10^{-3} S cm⁻¹ and a high Li⁺ migration number of 0.7 at room temperature and achieves stable cycling for over 2400 h in a symmetric lithium battery, as well as long-life operation with over 3300 cycles at -35 °C.

Additionally, the team demonstrated the compatibility of RMSPE with various high-voltage cathode materials (including LiCoO₂, LiNi_{0.8}Co_{0.1}Mn_{0.1}O₂, and LiFe_{1-x}Mn_xPO₄), confirming its potential for practical lithium metal battery applications.

Together, these works demonstrate how PIPS-enabled bicontinuous architectures can be precisely tailored through polymer chemistry and nanostructure design to simultaneously optimize electrochemical, mechanical, and interfacial properties of SPEs. The integration of phase behavior regulation and molecular design facilitates enhanced segmental relaxation within the polymer backbone and reduces the glass transition temperature, thereby promoting the rapid transport of lithium ions. This design strategy offers a novel approach for the development of advanced SPEs and contributes to a deeper understanding of the correlation between the microphase structure of polymer electrolytes and Li⁺ transport behavior.

3. Functional Design of Polymer Electrolytes

In the previous chapter, we systematically explored various key mechanisms in polymer electrolytes, revealing their importance to the ionic transport behavior, mechanical properties, and interface stability of the electrolytes. Based on these theoretical

foundations, we now shift our focus to how functional design can further optimize the performance of polymer electrolytes. Therefore, this chapter will systematically elaborate on the latest developments in the functional design of polymer electrolytes from three aspects: channel design, high-entropy design, and flame-retardant design. First, channel design significantly enhances the ionic conductivity and lithium ion migration number by constructing efficient ionic transport paths; second, high-entropy design, by introducing multiple components with specific functional groups, helps to improve the structural stability and electrochemical performance of the electrolyte; finally, flame-retardant design, by introducing flame retardants or designing self-extinguishing polymers, effectively improves the safety performance of the electrolyte. This chapter will delve into these functional design strategies, offering new insights for the development of high-performance SPEs.

3.1. Channel Design

In polymer electrolytes, ionic transport efficiency is one of the core factors determining their electrochemical performance. Traditional amorphous polymer electrolytes often exhibit low ionic conductivity due to the lack of ordered ionic transport pathways, limiting their application in high-performance batteries. Intentional design of ion channels can significantly increase ionic

conductivity and improve the utilization of active materials.^[99,100] This design strategy typically involves introducing functional fillers or functional groups into the polymer matrix to form directed ionic transport channels, thereby significantly lowering the energy barrier for ion migration and increasing lithium ion migration numbers. Through molecular design (such as block copolymers and graft copolymers) and the introduction of nanofillers (active fillers and inert fillers), precise control over the ionic transport channels can be achieved.^[101,102] Adding inert fillers (such as silica and alumina) or active fillers (such as $\text{Li}_{1.3}\text{Al}_{0.3}\text{Ti}_{1.7}(\text{PO}_4)_3$) into the polymer matrix can change the mobility of polymer chains through interactions with them, thereby improving ionic conductivity. Moreover, the active fillers themselves can also provide additional ionic transport pathways.

In general, ideal SPEs should have two types of Li^+ transport channels: one along the polymer chain, with a fast Li^+ migration rate and the other an internal cluster channel created by the solvation structure. If these two channels can work synergistically, rapid Li^+ diffusion dynamics may be achieved. Zhao et al.^[80] successfully developed a highly safe and flexible SPE by in situ polymerizing the acetylacetate allyl ester (AAA) monomer and visualized the construction of Li^+ transport channels with theoretical calculations (Figure 6a). Based on the polymerization of AAA monomers to prepare the polymer electrolyte, a layered SiO_2 with oxygen vacancies was prepared to effectively trap

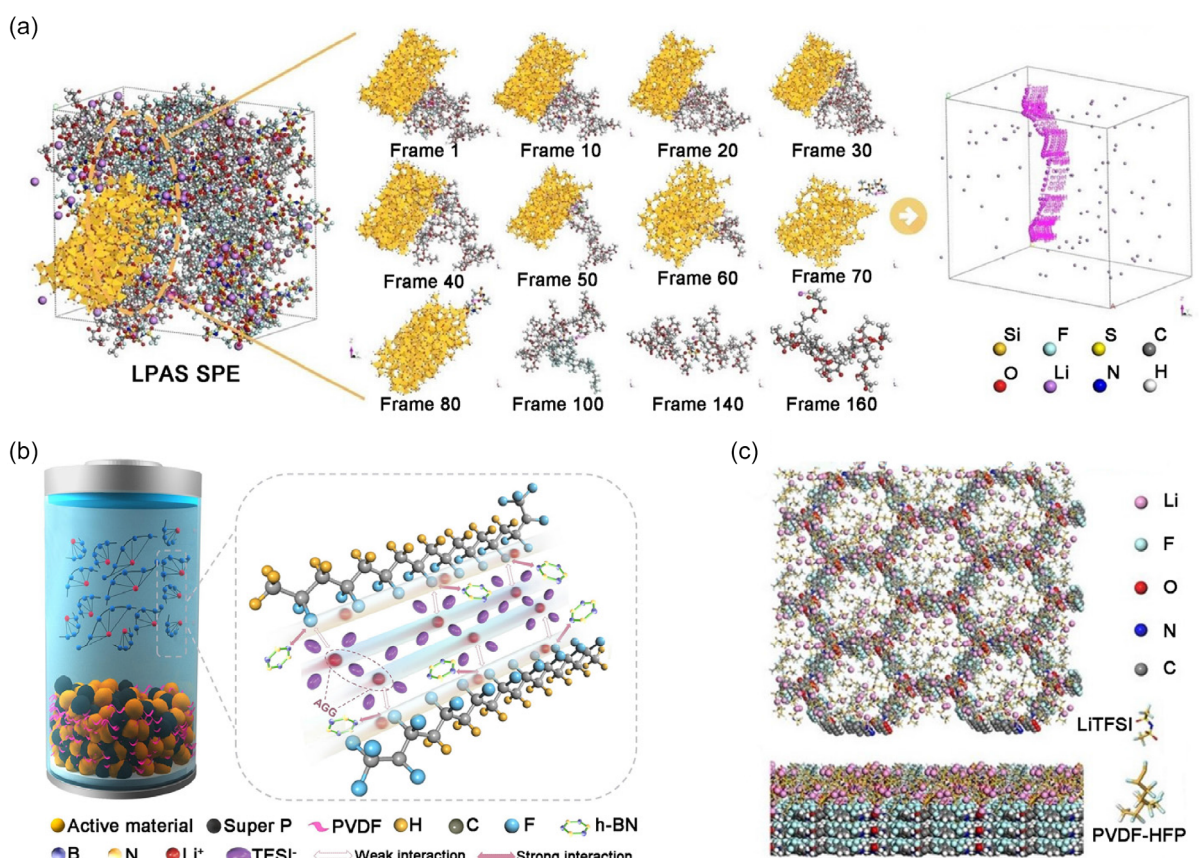


Figure 6. a) Visualization of Li^+ transport processes using the density field. Reproduced with permission.^[80] Copyright 2024, Wiley-VCH. b) Schematic representations of the Li^+ transport pathway in the designed PHLBH electrolyte. Reproduced with permission.^[103] Copyright 2023, Elsevier. c) Snapshot of Li-ion transport channels filled with $\text{CF}_3\text{-COF}$, derived from MD simulations. Reproduced with permission.^[104] Copyright 2024, Wiley-VCH.

TFSI⁻, allowing free Li⁺ to migrate quickly on the C=O active sites in polyacrylate (PAAA), building Li⁺ channels. This resulted in a room temperature ionic conductivity of 3.82×10^{-4} S cm⁻¹. Specifically, molecular dynamics simulations showed that effective Li⁺ channels were formed within the SPE. During the in situ polymerization, PVDF and P(VDF-HFP) were evenly distributed within the PAAA gaps. This electronegative band formed by the interaction of —F groups with —C=O and —C—O— groups acts as the Li⁺ transport channel. The electronegativity difference of the oxygen in the —C=O and —C—O— groups in PAAA serves as a gradient driving force, promoting Li⁺ migration. At the same time, after adding SiO₂, the Si atoms in SiO₂ acquire a positive charge and effectively bind with TFSI⁻. At the interface between the polymer and SiO₂, the oxygen atoms in SiO₂ accelerate Li⁺ migration by utilizing the different electronegativities formed by oxygen in PAAA, PVDF, and F in P(VDF-HFP). Wang et al.^[103] reported an SPE with dual Li⁺ channels (Figure 6b), i.e., PVDF-HFP/LiTFSI/BN (PHL_{1.25}BN₅). The interaction between the inorganic filler BN (boron nitride) and the —CF group in the polymer PVDF-HFP not only successfully accelerated the transport of Li⁺ along the polymer chain segments but also changed the solvation structure of Li⁺ in the electrolyte, forming a Li⁺ transport channel in the form of aggregated ion pairs (AGGs), thus accelerating the diffusion rate of Li⁺. Thanks to the AGG form of Li⁺ transport channels generated by BN, an SEI layer rich in inorganic components (LiF) was induced on the lithium metal surface, effectively inhibiting lithium dendrite growth while accelerating Li⁺ transport rate. As a result, the assembled Li/PHL_{1.25}BN₅/LFP full cell delivered a high discharge capacity of 156 mAh g⁻¹ and a Coulombic efficiency of 99.7% at 25 °C and 0.5 C. The specific discharge capacity of the Li/PHL_{1.25}BN₅/NCM523 full cell reached 140 mAh g⁻¹, and after 100 cycles at 0.5 C, the capacity retention was above 90%. Similarly, for channel design, Feng et al.^[104] proposed the design of ultrathin SPEs with long-range cooperative ion transport channels to effectively improve ionic conductivity and stability (Figure 6c). By immersing PVDF-HFP in the pores of a fluorinated covalent organic framework (CF₃-COF), the symmetry of the framework was disrupted, enabling rapid ion transport and suppressing anion migration. The introduction of CF₃-COF also enhanced the mechanical strength and flexibility of the SPE, ensuring uniform Li deposition and suppressing dendrite growth. As a result, a significantly high conductivity of up to 1.21×10^{-3} S cm⁻¹ was achieved. Ultimately, the ultrathin SPE demonstrated an ultralong cycle life of over 9000 h, and the NCM523/Li soft-pack battery also exhibited a high capacity of 760 mAh and a 96% capacity retention after cycling, bringing great promise for practical solid-state lithium metal battery applications. It is worth noting that, in addition to structural optimization of the fillers, the filler content also plays a critical role in the ion transport behavior within composite SPEs. An appropriate filler loading can effectively construct continuous ion-conduction pathways, enhance the mobility of polymer chains, and promote lithium salt dissociation, thereby improving ionic conductivity. However, if the filler content is too low, an interconnected conduction network may not form, limiting the enhancement effect. Conversely, an excessively high filler content can lead to particle agglomeration, increased interfacial resistance, and disruption of

the polymer matrix continuity, ultimately hindering ion transport. Therefore, optimizing the filler content to achieve a balance between mechanical reinforcement and ion conduction is essential. Filler loadings in the range of 5–20 wt% typically result in optimal electrochemical performance, although the exact value depends on the filler's type, morphology, and surface chemistry.

In summary, channel design provides a new dimension for the performance optimization of polymer electrolytes, with its core being the significant enhancement of ionic conductivity and lithium-ion transference number by constructing efficient ion transport pathways. Precise regulation of ion transport channels can promote rapid lithium-ion migration, anchor anions to reduce concentration polarization, and thereby enhance the overall electrolyte performance. Furthermore, the synergistic effect of the dual-channel design can also enhance the transmission dynamics of lithium ions. Future research should further explore the design and synthesis of novel functional fillers and groups, as well as the optimization of multichannel cooperative effects, providing breakthroughs for constructing high-speed lithium-ion channels.

3.2. High-Entropy Design

As an innovative material concept, high-entropy materials (HEMs) have recently attracted considerable attention in material science, with their utility extending to areas such as catalysis, thermoelectrics, and energy storage technologies. Unlike traditional materials, HEMs are usually single-phase, multicomponent (solid solution) materials, where the entropy-driven effect generated by the introduction of multiple elements plays a key role in enhancing performance.^[105–109] In practical applications, the high-entropy strategy can customize performance and break through the inherent limitations of battery materials.^[110] Generally, the Gibbs free energy is mainly affected by the competition between enthalpy change (ΔH) and entropy change (ΔS). By introducing multiple components to enhance the entropy change (ΔS), the negative impact of the increasing enthalpy change (ΔH) can be alleviated, thereby lowering the Gibbs free energy, and improving the stability and reaction rate of the electrolyte. Therefore, high-entropy electrolytes (HEEs) increase the system's disorder and complexity by integrating multiple elements.^[111–115] The unique characteristics of HEEs offer great potential for optimizing ionic conductivity, electrode/electrolyte interface properties, and battery stability.

High-entropy polymer electrolytes generally provide enhanced electrochemical stability windows and ionic conductivity characteristics. In general, high-entropy modification strategies for polymer matrices (such as blending, copolymerization, and grafting), salts, and inorganic fillers can suppress polymer crystallization and increase the amorphous phase ratio, thereby improving ionic conductivity. For SPEs with high-entropy polymer matrices, lithium-ion-conducting functional groups introduced by the high-entropy strategy can effectively promote lithium-ion migration in the molecular chains, thus enhancing ionic conductivity. To maximize the entropy of the electrolyte, Su et al.^[116] employed a synergistic strategy combining monomer modification, polymer

structure optimization, and chain-end engineering (**Figure 7a**) to successfully design a target-oriented high-performance SPE. Using atom transfer radical polymerization (ATRP), ring-opening polymerization, and click chemistry, they first constructed a high-entropy microdomain interlocking all-solid-state polymer electrolyte (HEMI-ASPE) with multifunctional ABC triblock copolymers (ABCTPs). Interestingly, in addition to the polymer chains and topology in specific regions, the customized star-shaped ternary copolymer also features specific terminal groups. Thanks to the terminal hydroxyl groups of the polylactic acid chains and the terminal bromine atoms of the polystyrene chains, the micronanoscale dynamic interpenetrating polymer network (dyn-IPN) in the target HEMI-ASPE successfully self-assembled and exhibited high topological entropy and excellent environmental adaptability. This strategy enables dyn-IPN to intelligently adjust the cross-linking density and form a 3D supramolecular polymer network. Furthermore, the terminal-modified methoxy-polyethylene glycol (MeOPEG) chains attached to the dyn-IPN backbone provide additional ionic conductivity, mainly due to their higher

molecular mobility. The resulting HEMI-ASPE exhibited excellent toughness ($6.72 \times 10^4 \text{ kJ m}^{-3}$), considerable ionic conductivity ($4.56 \times 10^{-4} \text{ S cm}^{-1}$ at 70°C), a high lithium-ion transference number ($t\text{Li}^+ = 0.63$). Based on these improvements, the Li/HEMI-ASPE/Li symmetric cell showed stable lithium plating/stripping performance for 4000 h. Similar progress was made in all-solid-state sodium metal batteries (AS-SMBs), further demonstrating the broad applicability of HEMI-ASPE as an advanced polymer material for battery chemistry. Similarly, Ye et al.^[117] designed a polycarbonate-based copolymer electrolyte (PCCE) with adjustable cation/anion solvation using a molecular enthalpy-entropy regulation strategy (**Figure 7b**). By adopting a copolymer system of cyclic and linear carbonates, they effectively reduced the cation-dipole interaction between lithium ions and carbonyl groups. This weak bonding (low enthalpy penalty) and nondirectional ion-dipole interactions allowed the cyclic and linear co-coordination system (high entropy penalty) to achieve weak solvation and rapid diffusion of lithium ions. Additionally, the polymer backbone introduced a methylene bisacrylamide

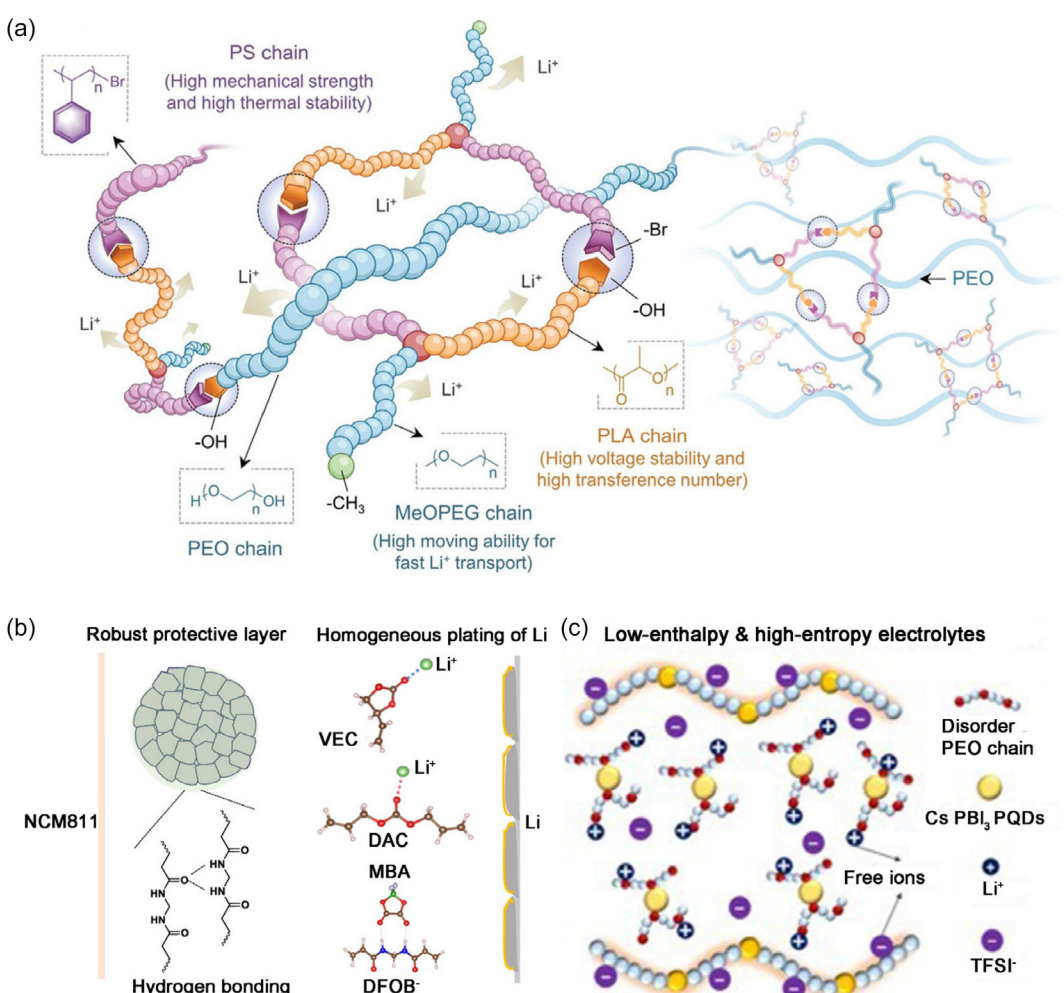


Figure 7. a) Schematic of the interactions within the HEMI-ASPE-Li membrane. Reproduced with permission.^[116] Copyright 2022, Wiley-VCH. b) Molecular design incorporating enthalpy–entropy manipulation for high-performance SPEs. Reproduced with permission.^[117] Copyright 2024, American Chemical Society. c) Schematic diagram of the LEHE electrolyte, with disordered PEO chains and enhanced free ion content due to the CsPbI₃ quantum strengthening of the PEO-LiTFSI complex. Reproduced with permission.^[118] Copyright 2022, Wiley-VCH.

crosslinking segment, which not only enhanced the mechanical strength of PCCE but also formed double hydrogen bonds with lithium salt anions. These double hydrogen bonds have strong bonding strength (high enthalpy penalty) and clear directionality (low entropy penalty), greatly limiting the free movement of anions. Therefore, based on this unique molecular structure design and optimization, the optimal PCCE exhibited high ionic conductivity of 0.66 mS cm^{-1} at 25°C , a Li^+ transference number of 0.76, and ultrahigh oxidation stability over 5.8 V. By using an *in situ* polymerization strategy, lithium metal batteries adapted to high-nickel $\text{LiNi}_{0.8}\text{Co}_{0.1}\text{Mn}_{0.1}\text{O}_2$ cathodes exhibited a capacity retention rate of 82.3% after 800 cycles at a cutoff voltage of 4.5 V, while lithium metal batteries adapted to $\text{LiNi}_{0.5}\text{Mn}_{1.5}\text{O}_4$ cathodes showed a capacity retention rate of 96.4% after 300 cycles at a cutoff voltage of 5.0 V. This molecular enthalpy-entropy regulation strategy provides new insights and molecular mechanisms for the design of high-voltage solid-state polymer electrolytes.

Introducing of inorganic fillers into SPEs can suppress the crystallization of polymer chains and increase the amorphous region, thereby improving ionic conductivity. However, traditional inorganic fillers (such as SiO_2 and Al_2O_3) have weak interactions with the polymer matrix, limiting the enhancement of conductivity. In contrast, high-entropy inorganic fillers can effectively address this issue by providing stronger interfacial interactions, significantly enhancing conductivity. Zhang et al.^[118] introduced CsPbI_3 perovskite quantum dots (PQDs) into PEO@LiTFSI composites (Figure 7c) to construct a low-enthalpy high-entropy (LEHE) SPE. After adding 1.5 wt% PQD filler, the diffusion coefficient of PEO-LiTFSI electrolyte increased from $1.76 \times 10^{-11} \text{ cm}^2 \text{ s}^{-1}$ to $2.75 \times 10^{-11} \text{ cm}^2 \text{ s}^{-1}$. After optimization, the room-temperature ionic conductivity of LEHE reached its highest value of $1.4 \times 10^{-4} \text{ S cm}^{-1}$ at the 1.5 wt% addition level. This improvement is attributed to the significant suppression of PEO chain crystallinity by CsPbI_3 quantum dots, which also endowed the PEO-LiTFSI- CsPbI_3 composite with high-entropy characteristics. As a result, the LEHE electrolyte exhibited extremely stable cycling performance, lasting over 1000 h. Moreover, the Li/LEHE/LiFePO₄ cell retained 92.3% of its initial capacity (160.7 mAh g^{-1}) after 200 cycles. Compared to the PEO@LiTFSI control group, the LEHE electrolyte significantly improved the lithium-ion transference number (0.57) and greatly reduced the activation energy for ion migration (0.14 eV).

High-entropy design, as an innovative material design strategy, provides new insights into the performance optimization of SPEs. By introducing the synergistic effects of multicomponent and multifunctional elements, high-entropy polymer electrolytes not only significantly enhance ionic conductivity and electrochemical stability but also improve electrode/electrolyte interfacial properties, thus laying the material foundation for next-generation high-energy-density and high-safety energy storage devices. From the structural optimization of polymer matrices to the interface regulation of inorganic fillers, the high-entropy design achieves precise control over the microstructure and macroscopic properties of the electrolyte by balancing enthalpy and entropy. However, more effort is still needed in the future, including the rational adjustment of polymer segments to further

enhance ionic conductivity and extend high-entropy SPEs for beyond-lithium batteries.

3.3. Flame Retardant Design

In LIBs, thermal runaway typically occurs in three key stages: heat generation, heat diffusion, and thermal runaway. In contrast, lithium-metal batteries (LMBs) face a more severe thermal runaway risk due to the highly reactive chemical activity of lithium metal. Research indicates that the electrolyte plays a critical role in this process. Therefore, developing electrolytes with high thermal stability and flame-retardant properties is a key measure to enhance battery safety.^[119–123] SPEs show great potential in significantly improving the safety of LMBs, primarily due to their excellent leakage prevention properties and the enhanced interfacial compatibility between electrode materials, which is improved by the introduction of plasticizers. However, the flammability of the polymer matrix in SPEs remains a serious safety concern. To address this challenge, it is necessary to develop intrinsically flame-retardant SPEs. This strategy mainly involves introducing efficient flame retardants into the plasticizer or chemically grafting flame-retardant functional groups directly onto the polymer backbone, thus constructing a fire barrier at the molecular level.^[124,125] The mechanisms of flame retardants mainly include gas-phase flame retardancy (such as releasing noncombustible gases to dilute oxygen), condensed-phase flame retardancy (such as forming a carbon layer to isolate heat), and interrupting free radical chain reactions, among others.^[126–129]

In recent years, researchers have successfully developed a series of polymer electrolytes with excellent flame-retardant properties through molecular design (such as the introduction of flame-retardant groups containing phosphorus, nitrogen, silicon, etc.) and composite techniques (such as adding nanoflame-retardant fillers). These designs not only significantly improve the thermal stability of the electrolyte but also maintain its electrochemical performance by optimizing interfacial compatibility. Li et al.^[130] successfully prepared a flame-retardant SPE (FRSPE) by *in situ* polymerization of a chemically bondable flame-retardant monomer (vinyl diethyl phosphate, DEVP) with methyl methacrylate (MMA) and allyl carbonate diethylene glycol (ADC) (Figure 8a). Specifically, their team used a phosphorus bonding strategy to effectively solve the problem of free flame-retardant molecules. First, chemically bonded phosphorus improves flame-retardant efficiency and achieves long-lasting flame retardancy, preventing the gradual consumption of flame-retardant molecules. Second, bonding the flame-retardant molecules to the polymer backbone effectively suppresses interface side reactions, eliminating ongoing side reactions between the flame-retardant molecules and lithium metal. Furthermore, the physical and chemical properties of the flame-retardant polymer solid electrolyte were evaluated and compared with FRGPE containing free flame-retardant molecules (triethyl phosphate (TEP)), revealing the superior performance of the bonded phosphorus electrolyte in terms of flame-retardant and electrochemical properties and discussing the mechanisms and reasons behind this. The results show that this FRSPE design effectively solves the problem of side

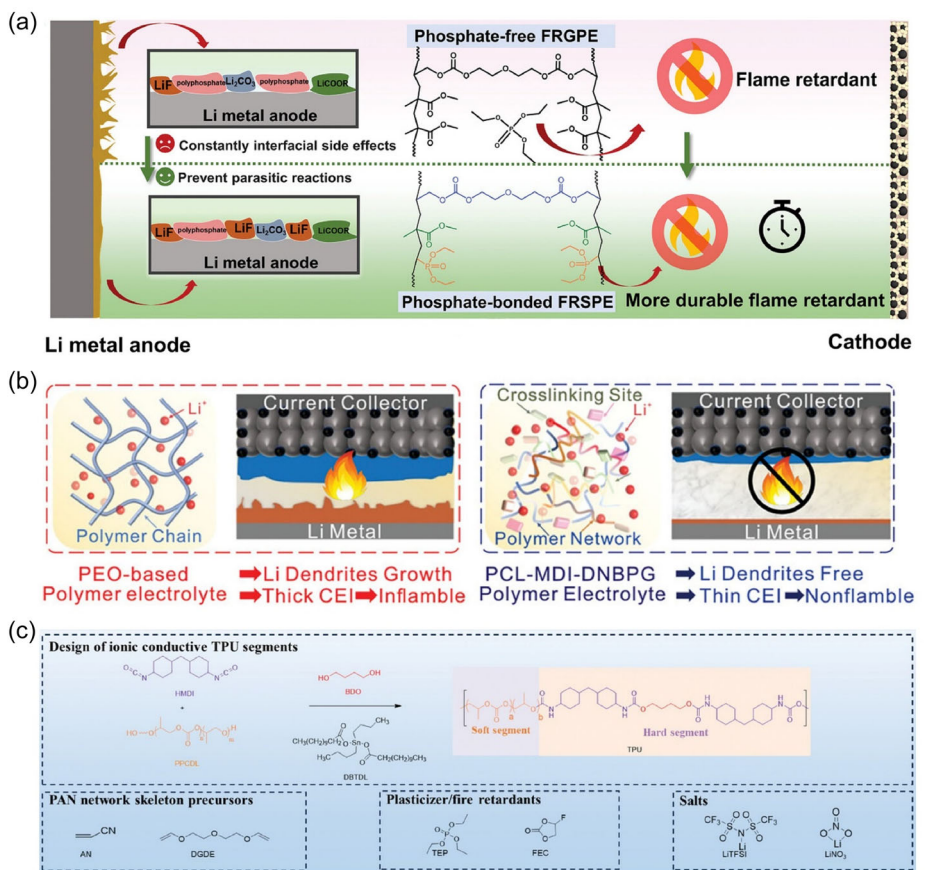


Figure 8. a) Schematic diagram comparing the phosphate-free FRGPE and the phosphate-bonded FRSPE. Reproduced with permission.^[130] Copyright 2024, Wiley-VCH. b) PEO-based polymer electrolyte and the nonflammable PCL-MDI-DBNPG electrolyte for lithium metal batteries. Reproduced with permission.^[20] Copyright 2023, Wiley-VCH. c) Schematic diagram of the TPU structure. Reproduced with permission.^[131] Copyright 2024, Wiley-VCH.

reactions between flame-retardant molecules and lithium metal, achieving efficient flame retardancy while exhibiting excellent electrochemical performance and safety under extreme conditions. Wu et al.^[20] designed and prepared PU-based SPEs with self-healing and flame-retardant properties through molecular design, selecting small molecules with different functions and using organic polymerization reactions (Figure 8b). The hydrogen bonds between ester groups ($-\text{COO}-$) and urethane groups ($-\text{NH}-\text{COO}-$) endow the electrolyte with excellent self-healing capabilities. At the same time, the introduced flame-retardant agents not only participated in the polymerization reaction but also acted as chain extenders to improve the mechanical strength of the polymer. Specifically, halogen-containing reactive flame-retardant agents were selected, and they were covalently bonded into the polymer backbone, effectively enhancing the flame-retardant performance of the solid electrolyte, and preventing ignition when exposed to an open flame. Additionally, these reactive flame-retardant agents also acted as chain extenders, giving the polymer electrolyte a high molecular weight ($M_w = 600\,000$) and excellent tensile performance ($>1400\%$). Similarly, Zhang et al.^[131] innovatively designed and synthesized a SIPN electrolyte framework with CO_2 -derived TPU as the main chain (Figure 8c). The electrolyte was constructed via an *in situ* polymerization process, where TPU as a hard segment provided abundant hydrogen

bonds, and the soft segments were rich in ion-complexation sites. Moreover, TPU has high oxidation stability, making it compatible with high-voltage cathode materials. By introducing triethylene glycol diacrylate as a crosslinking agent, a PAN-supported network was constructed, providing additional mechanical strength. The study also introduced TEP as a flame retardant and plasticizer. In the event of thermal runaway in the battery, TEP decomposes to generate phosphorus-containing free radicals, effectively interrupting the combustion process and ensuring that the electrolyte's self-extinguishing time does not exceed 5 s.

In summary, flame-retardant design plays a crucial role in enhancing the safety of LMBs. Through innovative molecular design and composite techniques, researchers have successfully developed FRSPEs with excellent properties. These electrolytes not only improve thermal stability and suppress side reactions with lithium metal but also enhance the electrochemical performance of the battery through structural optimization. However, despite the progress made, the research on FRSPEs still faces challenges in performance optimization and practical applications, especially in terms of stability and ionic conductivity at high and low temperatures. Therefore, future research should further explore the synergistic effects of flame-retardant agents and electrolyte matrices and improve the adaptability of the electrolyte under extreme conditions to meet the demands of

high-performance lithium metal batteries. Meanwhile, to achieve fully safe and reliable operation, several core issues must be addressed. First, a deeper understanding of thermal runaway mechanisms in LMBs is needed, particularly the impact of "dead lithium" formation at the anode during cycling. Second, enhancing the high- and low-temperature adaptability of FRSPEs and mitigating performance degradation are critical for improving battery stability. Finally, although advances in FRSPEs have improved ionic conductivity, further optimization to surpass liquid electrolytes while ensuring system safety remains a major research focus.

4. Interface Design

Despite the strong development momentum of solid-state lithium metal batteries, their commercialization process is constrained by major safety issues, especially the formation of dendrites and mossy metal deposits on the lithium metal anode, which can lead to internal short circuits, triggering fires and explosions. In addition, the formation of lithium dendrites between the electrolyte and the anode can significantly reduce Coulombic efficiency, severely affecting battery stability. Therefore, a special interface design is needed to optimize the physicochemical properties of the electrode–electrolyte interface,

thereby improving the cycling performance and safety of the battery. This chapter will systematically elaborate on the latest advances in interface design from the perspectives of artificial interface design and *in situ* interface design.

4.1. Artificial Interface Design

Artificially constructing interface protection layers with a wide electrochemical stability window is an effective method to address interface chemistry/electrochemical issues. Their main function is to act as a protective passivation layer, preventing direct contact between electrode materials and electrolytes, thereby preventing side reactions at the interface during electrochemical cycling.^[132–135] In addition, in some systems, interface protection layers can also suppress the formation of space charge layers (SCL) and the diffusion of elements. Common interface protection layer materials include metal oxides, inorganic ionic conductors, and polymer materials.^[135–138]

Notably, the designed artificial interface can also better form efficient and stable SEI. Zhao and others^[139] modified the interface between the polymer electrolyte and the anode using silk fibroin peptide (SFP) and MXene, constructing an artificial interface layer of about 5 μm (Figure 9a,b). The —NH₂ groups in SFP and the —F terminal in MXene promoted the formation of Li₃N

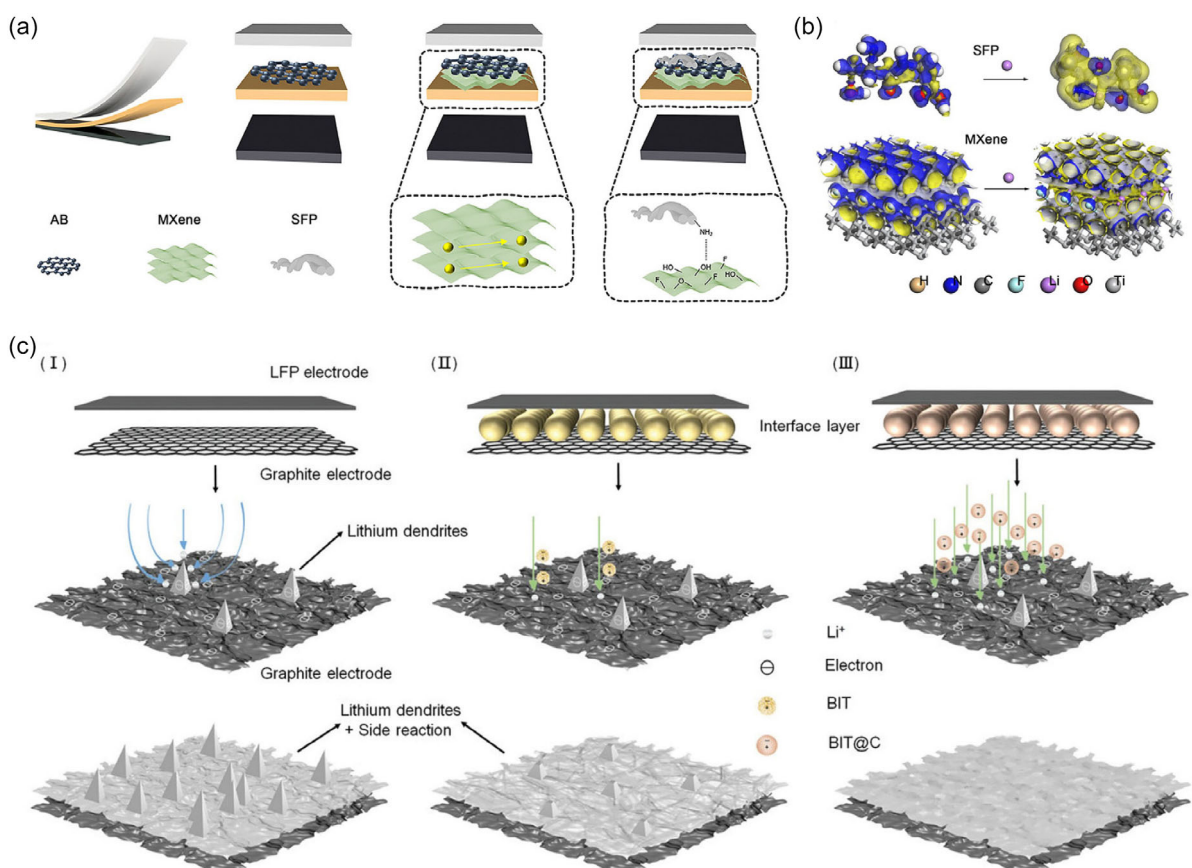


Figure 9. a) Schematic representation of various modified interfaces in SLIBs. b) Charge density difference of adsorbed Li⁺ on SFP and MXene, respectively. Reproduced with permission.^[139] Copyright 2023, Elsevier. c) Schematic representation of different modified interfaces in LIBs. Reproduced with permission.^[140] Copyright 2024, Wiley-VCH.

and LiF, achieving selective regulation of the SEI membrane growth with beneficial components. TOF-SIMS and AFM-DMT confirmed that the SEI membrane containing Li₃N and LiF components formed uniformly and remained stable. This not only enhanced interface stability but also induced uniform nucleation of lithium ions, suppressed dendrite growth, and improved the electrochemical performance of the battery. Furthermore, DFT calculations determined the lithium-ion adsorption model and its related adsorption energy and visually revealed the charge density distribution during the interaction process between lithium ions and SFP or MXene-F. After adsorption, positive charges were accepted by the N atoms in SFP or the F atoms in MXene-F and accumulated between the lithium ions and —N, as well as between the lithium ions and —F, forming two highly adaptive SEI membranes, LiF and Li₃N. Therefore, the ion conductivity of the prepared polymer electrolyte reached 1.16×10^{-3} S cm⁻¹, and the lithium-ion transference number was 0.57. Notably, the assembled LiFePO₄ battery demonstrated an initial room temperature discharge capacity of 117.6 mAh g⁻¹ under 5 C conditions. Similarly, Li and his team^[140] added a ferroelectric-modified layer (BIT@C) between the anode and SPE, improving the cycle stability of lithium batteries at room temperature by reducing the harm of SCL and promoting the uniform and rapid transport of interface lithium ions (Figure 9c). The ferroelectric interface generated a reverse polarization electric field, effectively maintaining the consistency of the electric field and ion concentration distribution between the graphite anode and SPE. Additionally, the BIT@C intermediate film facilitated the 3D nucleation of lithium ions and horizontal (2D) extension, significantly reducing the interface resistance, maintaining the stability of the SEI membrane, protecting the structural integrity of the graphite anode, and enabling fast interface ion conduction, thereby achieving long-term stable cycling performance at room temperature. In short, ferroelectric materials help open lithium-ion channels at the solid-solid interface of solid-state full batteries, achieving uniform intercalation performance of lithium ions through the reverse polarization electric field. Notably, the lithium-ion transference number achieved with the BIT@C artificial interface layer was an impressive 0.72. Furthermore, the assembled full battery exhibited stable cycling performance at 2 C (120.4 mAh g⁻¹) at room temperature, maintaining a specific discharge capacity of 80.1 mAh g⁻¹ after 1200 cycles. This ferroelectric-modified intermediate film provides an effective strategy for constructing uniform ion channels and minimizing undesirable side reactions at the interface.

Collectively, it can be concluded that both chemical modification using functional groups to tailor the SEI composition and physical modulation via polarized fields to enhance the uniformity of ion flux contribute to the construction of stable and high-performance interfaces in solid-state lithium batteries. Although these strategies are based on different mechanisms, they share a common direction—namely, that tuning the properties of artificial interfaces can effectively regulate SEI formation and promote uniform Li⁺ deposition. Their complementarity underscores the importance of integrating chemical regulation with physical design for the rational development of high-performance interfacial architectures in solid-state lithium batteries.

4.2. In Situ Interface Design

In addition to artificially constructing a pre-existing interface layer on the material surface, another effective strategy is to introduce additives or grafted groups into the solid-state electrolyte to in situ generate an interface protection layer. This method not only effectively prevents interface side reactions but also reduces the need for additional interface construction steps, thereby lowering costs.^[141–148]

Recent studies by Li et al.^[149] have shown that ion nanoclusters self-assembled between lithium ions and rigid rod-like sulfonated aromatic polyamides (poly 2,2'-disulfonyl-4,4'-benzidine terephthalamide, PBDT) contribute to uniform lithium deposition and significantly reduce interfacial charge transfer resistance, achieving a reduction of 102–103 times compared to PEO-based electrolytes (Figure 10a). Furthermore, this design effectively suppresses the growth of lithium dendrites. Batteries assembled with this SPE exhibit a record-high critical current density ($6 \text{ mA cm}^{-2/3} \text{ mAh cm}^{-2}$) at room temperature, and after 10 000 cycles with a lithium iron phosphate cathode (under 5 C conditions), the capacity retention reached 80%. When the temperature is raised to 80 °C, the battery maintains nearly 100% of its theoretical capacity under 3 C conditions and exhibits a high specific power density (20 kW kg⁻¹). Through cryo-electron microscopy imaging and computational simulations, it was found that these self-assembled ion nanoclusters promote ultrafast charge transfer dynamics by balancing the pre-exponential factor and activation energy of the lithium-polymer space charge interface, thereby enhancing the interfacial charge transfer efficiency. This interfacial design strategy leverages the thermodynamically favorable interactions of ion binding and self-assembly between metal ions and polyanions, ensuring excellent charge transfer dynamics in solid-state polymer lithium metal batteries. Ma et al.^[150] designed a double-layer heterogeneous structure of SPEs by directly curing functional boron-containing monomers on the electrode surface to ensure excellent conductivity and address interfacial issues, thus achieving long-lasting high-voltage tolerance and suppressing lithium dendrite growth (Figure 10b). The unoccupied p-orbitals in the 3D crosslinked network of the electrolyte not only improve the transfer number of Li⁺ (0.78) but also enhance the interfacial stability of lithium metal and suppress dendrite growth by anchoring PF₆⁻ anions and regulating uniform lithium deposition, thereby ensuring the long cycling performance of Li/BGPE/Li batteries. Additionally, functional additives such as tri(trimethylsilyl)phosphite and tris(pentafluorophenyl)borane can preferentially oxidize and decompose, in situ forming a stable SEI layer rich in B, F, and Si, which effectively promotes the uniform growth of the SEI. Based on this in situ interfacial design strategy, full cells paired with LiNi_{0.5}Co_{0.2}Mn_{0.3}O₂ and LiFePO₄ cathodes have demonstrated excellent stable cycling and superior rate performance. Zhang et al.^[136] proposed a molecular crowding strategy to adjust the Li⁺ coordination structure, thus in situ modulating the interfacial chemical properties to stabilize the electrode/electrolyte interface of ASSLMB (Figure 10c). Based on a molecular structure similar to poly(ethylene oxide) chains and weak supramolecular interactions with lithium ions, 15-crown-5 was introduced into

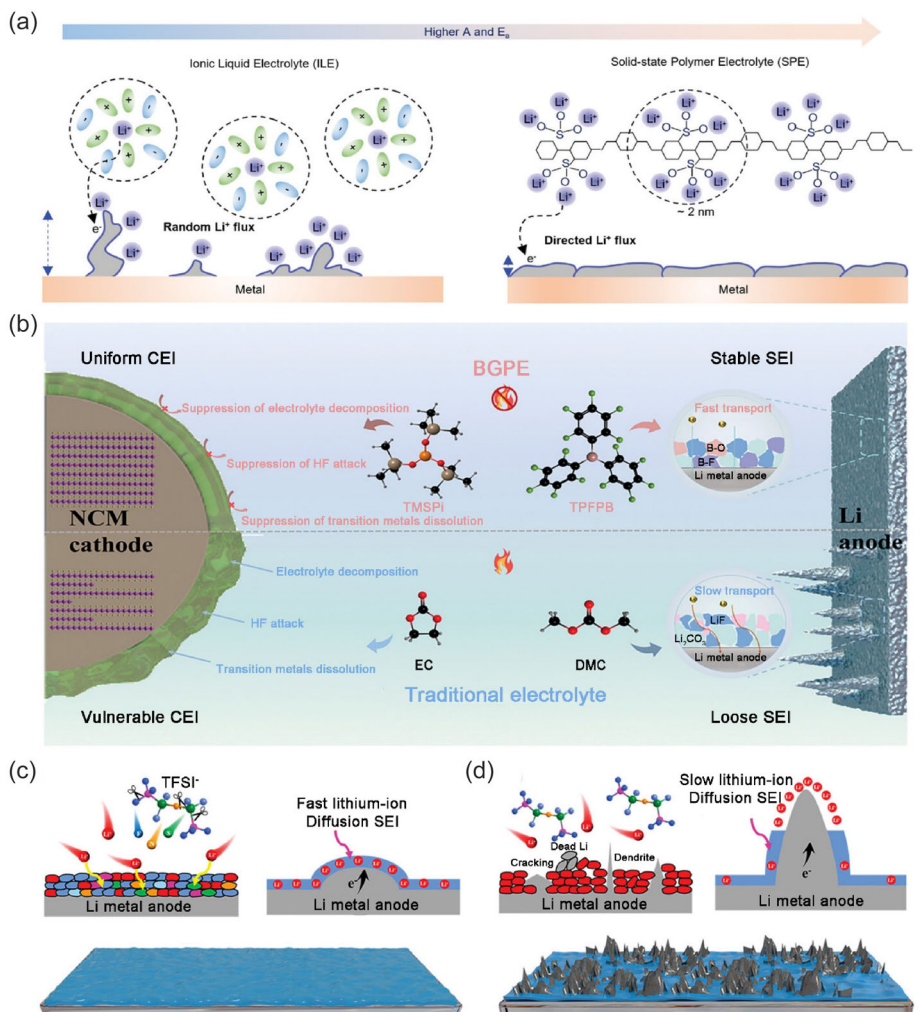


Figure 10. a) Schematic representation of charge-transfer processes and lithium deposition at the electrolyte-electrode interfaces in ILEs and SPEs with polyanions containing SO_3^- groups. Reproduced with permission.^[149] Copyright 2024, Wiley-VCH. b) Design diagram depicting the multifunctional mechanism of BGPE. Reproduced with permission.^[150] Copyright 2024, Wiley-VCH. c,d) Schematic representation of the lithium deposition mechanism with PEOC15 and PEO electrolytes. Reproduced with permission.^[136] Copyright 2024, Wiley-VCH.

the SPE to disrupt the crystallinity of the polymer matrix and facilitate the dissociation of lithium salts. Due to the good compatibility of 15-crown-5 with polyethylene oxide and its electrostatic repulsion toward TFSI^- anions, the enriched anions are forced to be confined within the Li^+ coordination sheath, thereby weakening the coordination between Li^+ and the $-\text{CH}_2\text{CH}_2\text{O}-$ (EO) groups in polyethylene oxide, thus promoting Li^+ transport. The reduction of closed anions is enhanced, and anions are easily decomposed at the electrolyte-anode interface, forming an SEI rich in LiF , which accelerates Li^{+} diffusion and facilitates uniform lithium deposition. The inorganic content in the SEI increases Young's modulus, thereby preventing dendrite growth and interface penetration. Therefore, symmetric LIBs using polyethylene oxide electrolyte doped with 15-crown-5 (PEOC15) can operate ultrastably for about half a year, with the assembled all-solid-state LFP/PEOC15/Li full battery exhibiting high rate and long cycle life characteristics. The capacity retention of the $\text{LiNi}_{0.8}\text{Co}_{0.1}\text{Mn}_{0.1}\text{O}_2/\text{PEOC15/Li}$ full battery under high voltage cycling is also satisfactory. Notably, by using this easily available and large-scale prepared SPE, pouch batteries show excellent flexibility and stability.

In summary, the mainstream solutions to the chemical/electrochemical interface issue include artificially generated interfacial protective layers and *in situ* constructed interfacial layers. These strategies are typically effective in suppressing side reactions caused by the narrow electrochemical window, preventing element diffusion, and avoiding space charge layer effects. In the protective layer strategy, the ideal interfacial protective layer should possess good ionic conductivity and excellent mechanical properties. Compared to artificially generated interfacial layers, *in situ* formed layers require no additional manufacturing steps, are simpler to operate, and are better suited for large-scale production. However, artificially generated layers offer greater controllability and more effectively suppress lithium dendrite growth, suggesting broader future applicability.

5. Conclusion and Outlook

Electrolyte design is crucial for the development of advanced batteries with outstanding performance. This review summarizes the

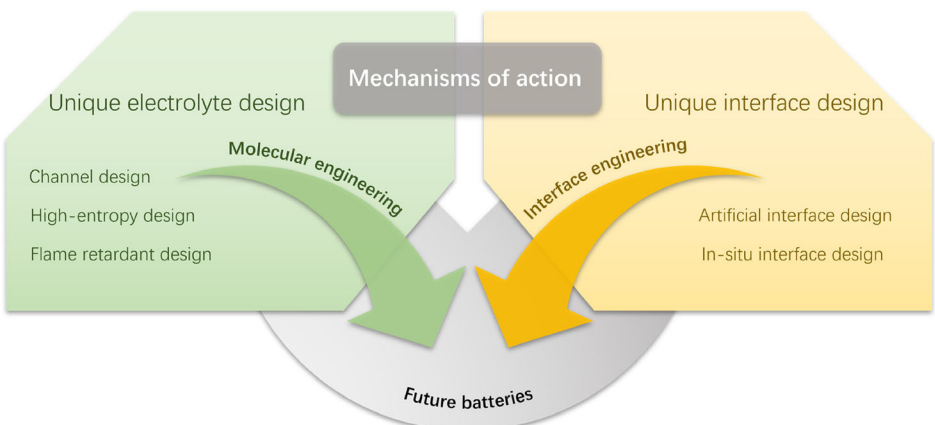


Figure 11. Overview diagram of summary and prospects.

key mechanisms of SPEs in solid-state batteries and their functional design strategies (Figure 11). Firstly, the ion transport mechanisms and various interactions in SPEs are discussed from four aspects: Lewis acid-base theory, anion vacancies, hydrogen bonding networks, and phase separation structures. Research has shown that regulating these microscopic interactions can significantly improve the ionic conductivity and interfacial stability of SPEs. In particular, the introduction of functional fillers and the application of molecular design approaches have provided new ways to optimize ionic conductivity and ion migration numbers. Secondly, three advanced functional design strategies are introduced in detail: channel design, high-entropy design, and flame-retardant design. Channel design significantly enhances ionic conductivity by constructing directed ion transport pathways; high-entropy design utilizes the synergistic effect of multicomponents to enhance the structural stability and electrochemical performance of the electrolyte; flame retardant design improves electrolyte safety through molecular design (introducing flame-retardant elements such as phosphorus, nitrogen, and silicon) and composite techniques (introducing flame-retardant fillers). These strategies not only effectively address the practical challenges of SPEs but also lay the foundation for the development of high-performance solid-state batteries. Finally, regarding the electrode/electrolyte interface issue, we discuss artificial interface design and in situ interface design strategies. By reasonably designing interfacial protective layers, lithium dendrite growth can be suppressed, and interface stability can be improved, thereby enhancing the cycle life and safety of the battery.

To guide the design of electrolytes and interfaces for the next generation of high-energy-density and high-safety batteries, we propose that future efforts should be directed toward the following key objectives. i) Achieving an optimal balance between ionic conductivity and mechanical properties. While high ionic conductivity is critical for efficient ion transport, sufficient mechanical strength is essential to suppress dendrite growth and ensure structural integrity. Future research should explore strategies such as the rational design of HEMs, the incorporation of multifunctional nanofillers, and the optimization of phase-separated structures to simultaneously enhance these two aspects. ii) Improving interfacial stability. Although various interface engineering approaches have

been developed, interfacial side reactions, especially under long-term cycling and practical operating conditions, remain a major challenge. Therefore, future work should focus on developing robust and self-healing interfacial protective layers, as well as investigating the dynamic evolution of interfaces at the atomic and molecular levels during electrochemical processes, using advanced *in situ* characterization techniques. iii) Enhancing adaptability under extreme conditions. In practical applications, batteries are often exposed to harsh environments such as high or low temperatures. To address this, SPEs with higher thermal stability, wider operational temperature ranges, and excellent mechanical resilience need to be designed. This may involve the development of novel polymer matrices with intrinsic temperature resistance, the design of supramolecular structures, or the introduction of smart functional groups that respond adaptively to environmental changes. iv) Promoting cost-effectiveness and scalability. Although many advanced electrolyte and interface design strategies have shown impressive laboratory-scale performance, their complexity, high material costs, and intricate fabrication processes hinder large-scale commercialization. Therefore, future research should prioritize the discovery of low-cost raw materials, the simplification of synthesis procedures, and the development of scalable manufacturing technologies. Additionally, interdisciplinary collaboration will be crucial for accelerating progress; in particular, the integration of solid-state battery research with artificial intelligence, machine learning, and computational modeling could greatly enhance material discovery, interface design, and performance optimization. By addressing these challenges systematically, it is expected that the practical application of next-generation solid-state batteries can be significantly advanced.

Acknowledgements

We acknowledge the funding support by the Heilongjiang Provincial Natural Science Foundation of China (LH2024B017), the Harbin Manufacturing Science and Technology Innovation Talent Project (2022CXRCCG007), the Heilongjiang Province Ecological Environment Protection Research Project (HST2022DQ007), and the National Natural Science Foundation of China (21706043).

Conflict of Interest

The authors declare no conflict of interest.

Author Contributions

Wenhai Xu: formal analysis (lead); investigation (lead); methodology (lead); validation (lead); Visualization (lead); writing—original draft (lead); writing—review and editing (lead). **Libo Li:** funding acquisition (lead); project administration (lead); resources (lead); supervision (lead); writing—review and editing (equal). **Hang Yang:** software (equal). **Suo Li:** investigation (supporting). **Zhixuan Wang:** investigation (supporting).

Keywords: action mechanisms • electrolyte designs • interface designs • lithium-metal batteries • solid-state polymer electrolytes

- [1] H. Yang, Y. Zhao, S. Li, H. Tong, L. Li, *Batteries Supercaps* **2024**, 7, e202400039.
- [2] S. Li, L. Li, H. Yang, Y. Zhao, Y. Shan, *Chem. Eng. J.* **2024**, 484, 149433.
- [3] H. Tong, L. Li, Y. Zhao, Y. Zhang, H. Yang, S. Li, Z. Wang, W. Xu, *Energy Storage Mater.* **2025**, 76, 104100.
- [4] F. Schomburg, B. Heidrich, S. Wennemar, R. Drees, T. Roth, M. Kurrat, H. Heimes, A. Jossen, M. Winter, J. Y. Cheong, F. Röder, *Energy Environ. Sci.* **2024**, 17, 2686.
- [5] Z. Wang, H. Yang, S. Li, H. Tong, W. Xu, Y. Zhao, L. Li, *Energy Mater.* **2024**, 4, 400080.
- [6] S. Dong, L. Shi, S. Geng, Y. Ning, C. Kang, Y. Zhang, Z. Liu, J. Zhu, Z. Qiang, L. Zhou, G. Yin, D. Li, T. Mu, S. Lou, *Nano-Micro Lett.* **2025**, 17, 95.
- [7] D. Witt, L. Bläubaum, F. Baakes, U. Krewer, *Batteries Supercaps* **2024**, 7, e202400023.
- [8] J. Chen, K. Hu, Z. Wang, H. Xu, Y. Huang, X. Hu, *Small* **2025**, 21, 2410118.
- [9] C. Liu, X. Huang, X. Yu, Z. Wang, Y. Shen, S. Yuan, Y. Wang, *Angew. Chem. Int. Edit.* **2025**, 64, e202415915.
- [10] H. Li, D. Shimizu, R. Jin, T. Zhang, D. Horikawa, K. Nagaya, H. Tsubouchi, H. Yamaguchi, M. Okumura, T. Ichitsubo, *J. Mater. Chem. A* **2025**, 13, 3619.
- [11] Y. Pu, Y. Zhang, K. Zhan, Q. Zhang, T. Qin, X. Yang, X. Luo, X. Zeng, W. Yang, Y. Zhang, X. Li, *Small Methods* **2024**, 2401936, <https://doi.org/10.1002/smtd.202401936>.
- [12] A. Chauhan, C. Lischka, H. Nirschl, *Batteries Supercaps* **2024**, 7, e202400051.
- [13] Q. Cai, G. Li, D. Kong, J. Xu, J. Cai, Z. Xie, H. Liu, L. Xing, W. Li, *Chem. Eng. J.* **2025**, 505, 159156.
- [14] C. Yan, W. Li, Z. Liu, S. Zheng, Y. Hu, Y. Zhou, J. Guo, X. Ou, Q. Li, J. Yu, L. Li, M. Yang, Q. Liu, F. Yan, *Adv. Funct. Mater.* **2024**, 34, 2314408.
- [15] J. Dong, L. Li, Y. Niu, Z. Pan, Y. Pan, L. Sun, L. Tan, Y. Liu, X. Xu, X. Guo, Q. Wang, H. Wang, *Adv. Energy Mater.* **2024**, 14, 2303732.
- [16] S. Oh, A. R. Jeon, G. Lim, M. K. Cho, K. H. Chae, S. S. Sohn, M. Lee, S. K. Jung, J. Hong, *Energy Storage Mater.* **2024**, 65, 103169.
- [17] H. Y. Liu, X. Y. Liu, N. Zhang, P. F. Wang, Z. L. Liu, J. Shu, T. F. Yi, *J. Energy Chem.* **2025**, 101, 68.
- [18] L. Wheatcroft, A. Bird, N. Gollapally, S. G. Booth, S. A. Cussen, B. J. Inkson, *Batteries Supercaps* **2024**, 7, e202400077.
- [19] C. Xu, X. Liu, O. Sumińska-Ebersoldt, S. Passerini, *Batteries Supercaps* **2024**, 7, e202300590.
- [20] L. Wu, F. Pei, D. Cheng, Y. Zhang, H. Cheng, K. Huang, L. Yuan, Z. Li, H. Xu, Y. Huang, *Adv. Funct. Mater.* **2024**, 34, 2310084.
- [21] Y. Li, J. Li, Y. Ding, X. Feng, X. Liu, P. Yan, M. Sui, M. Ouyang, *Energy Storage Mater.* **2024**, 65, 103167.
- [22] N. LeGe, X. He, Y. X. Wang, Y. Lei, Y. X. Yang, J. T. Xu, M. Liu, X. Wu, W. H. Lai, S. L. Chou, *Energy Environ. Sci.* **2023**, 16, 5688.
- [23] T. Deng, C. Wang, H. Wan, A. Li, X. He, Z. Wang, L. Cao, X. Fan, C. Wang, *Angew. Chem. Int. Edit.* **2025**, 64, e202418811.
- [24] X. Lin, M. Wang, J. Zhao, X. Wu, J. Xie, J. Yang, *Carbohydr. Polym.* **2023**, 304, 120502.
- [25] L. Liu, H. Zschiesche, M. Antonietti, M. Gibilaro, P. Chamelot, L. Massot, P. Rozier, P. Taberna, P. Simon, *Adv. Energy Mater.* **2023**, 13, 2203805.
- [26] X. Xia, S. Xu, F. Tang, Y. Yao, L. Wang, L. Liu, S. He, Y. Yang, W. Sun, C. Xu, Y. Feng, H. Pan, X. Rui, Y. Yu, *Adv. Mater.* **2023**, 35, 2209511.
- [27] Q. Liu, X. Wang, *Angew. Chem. Int. Edit.* **2023**, 62, e202217764.
- [28] M. Celik, S. Pakseresht, A. W. M. Al-Ogaili, S. Usta, H. Akbulut, T. Cetinkaya, *Batteries Supercaps* **2023**, 6, e202300263.
- [29] Q. Xu, Z. Liu, Y. Jin, X. Yang, T. Sun, T. Zheng, N. Li, Y. Wang, T. Li, K. Wang, J. Jiang, *Energy Environ. Sci.* **2024**, 17, 5451.
- [30] X. Cheng, Y. Jiang, C. Lu, J. Li, J. Qu, B. Wang, H. Peng, *Batteries Supercaps* **2023**, 6, e202300057.
- [31] Y. H. T. Tran, K. An, D. T. T. Vu, S. W. Song, *ACS Energy Lett.* **2025**, 10, 356.
- [32] Y. Lou, Z. Lin, J. Shen, J. Sun, N. Wang, Z. Chen, R. Huang, X. Rui, X. Wu, H. Yang, Y. Yu, *Adv. Mater.* **2025**, 37, 2416136.
- [33] N. R. Park, Y. Li, W. Yao, M. Zhang, B. Han, C. Mejia, B. Sayahpour, R. Shimizu, B. Bhawmala, B. Dang, S. Kumakura, W. Li, Y. S. Meng, *Adv. Funct. Mater.* **2024**, 34, 2312091.
- [34] J. Huang, B. Hu, J. Meng, T. Meng, W. Liu, Y. Guan, L. Jin, X. Zhang, *Energy Environ. Sci.* **2024**, 17, 1007.
- [35] T. Kim, *J. Mater. Chem. A* **2024**, 12, 2902.
- [36] X. Xue, C. Li, Z. Shangguan, C. Gao, K. Chenhai, J. Liao, X. Zhang, G. Zhang, D. Zhang, *Adv. Sci.* **2024**, 11, 2305800.
- [37] K. Daems, P. Yadav, K. B. Dermeinci, J. Van Mierlo, M. Berecibar, *Renew. Sustain. Energy Rev.* **2024**, 191, 114136.
- [38] Y. Wang, Z. Wu, F. M. Azad, Y. Zhu, L. Wang, C. J. Hawker, A. K. Whittaker, M. Forsyth, C. Zhang, *Nat. Rev. Mater.* **2023**, 9, 119.
- [39] F. Yang, D. Wang, Z. Zhang, X. Tai, M. Qiu, X. Fu, *Energy Storage Mater.* **2024**, 65, 103134.
- [40] M. Sun, Z. Zeng, W. Zhong, Z. Han, L. Peng, S. Cheng, J. Xie, *Batteries Supercaps* **2022**, 5, e202200338.
- [41] M. K. Bera, S. Sarmah, D. C. Santra, M. Higuchi, *Coord. Chem. Rev.* **2024**, 501, 215573.
- [42] P. Yadav, P. Thakur, D. Maity, T. N. Narayanan, *Small* **2024**, 20, 2308344.
- [43] Y. Sun, J. Li, S. Xu, H. Zhou, S. Guo, *Adv. Mater.* **2024**, 36, 2311687.
- [44] F. Li, X. Cheng, G. Lu, Y. C. Yin, Y. C. Wu, R. Pan, J.-D. Luo, F. Huang, L.-Z. Feng, L.-L. Lu, T. Ma, L. Zheng, S. Jiao, R. Cao, Z.-P. Liu, H. Zhou, X. Tao, C. Shang, H.-B. Yao, *J. Am. Chem. Soc.* **2023**, 145, 27774.
- [45] C. Ciarlantini, I. Francolini, I. Silvestro, A. Mariano, A. Scotto d'Abusco, A. Piozzi, *Carbohydr. Polym.* **2024**, 327, 121684.
- [46] X. Wang, D. Guan, C. Miao, J. Li, J. Li, X. Yuan, X. Ma, J. Xu, *Adv. Energy Mater.* **2024**, 14, 2303829.
- [47] J. Biao, C. Bai, J. Ma, M. Liu, F. Kang, Y. Cao, Y. He, *Adv. Energy Mater.* **2024**, 14, 2303128.
- [48] S. Kim, Y. Lee, K. Kim, B. C. Wood, S. S. Han, S. Yu, *ACS Energy Lett.* **2024**, 9, 38.
- [49] Z. Ye, S. Zhai, R. Liu, M. Liu, Y. Xu, C. Li, X. Wang, T. Mei, *Chem. Eng. J.* **2024**, 479, 147847.
- [50] J. Wei, P. Zhang, T. Shen, Y. Liu, T. Dai, Z. Tie, Z. Jin, *ACS Energy Lett.* **2023**, 8, 762.
- [51] Z. Lin, G. Fan, T. Zhang, F. Huo, Q. Xi, J. Wang, T. She, X. Zeng, J. Weng, W. Huang, *Adv. Energy Mater.* **2023**, 13, 2203532.
- [52] L. Wang, S. Xu, Z. Wang, E. Yang, W. Jiang, S. Zhang, X. Jian, F. Hu, *eScience* **2023**, 3, 100090.
- [53] B. Li, P. F. Cao, T. Saito, A. P. Sokolov, *Chem. Rev.* **2023**, 123, 701.
- [54] H. J. Shin, S. Park, S. Park, D. Kim, *Adv. Sci.* **2023**, 10, 2205424.
- [55] S. De, S. J. Rukmani, X. Zhao, C. Clarkson, F. Vautard, S. Bhagia, M. Goswami, S. Zhang, S. F. Elyas, W. Zhao, J. C. Smith, A. J. Ragauskas, S. Ozcan, H. Tekinalp, M. Si, J. Huang, X. He, *Adv. Funct. Mater.* **2025**, 35, 2414222.
- [56] J. Li, A. Azizi, S. Zhou, S. Liu, C. Han, Z. Chang, A. Pan, G. Cao, *eScience* **2024**, 5, 100294.
- [57] S. C. Sand, J. L. M. Rupp, B. Yildiz, *Chem. Soc. Rev.* **2025**, 54, 178.
- [58] L. Ye, X. Li, *Nature* **2021**, 593, 218.
- [59] Z. Ning, G. Li, D. L. R. Melvin, Y. Chen, J. Bu, D. Spencer-Jolly, J. Liu, B. Hu, X. Gao, J. Perera, C. Gong, S. D. Pu, S. Zhang, B. Liu, G. O. Hartley, A. J. Bodey, R. I. Todd, P. S. Grant, D. E. J. Armstrong, T. J. Marrow, C. W. Monroe, P. G. Bruce, *Nature* **2023**, 618, 287.
- [60] L. Ye, Y. Lu, Y. Wang, J. Li, X. Li, *Nat. Mater.* **2024**, 23, 244.
- [61] C. Li, S. Zhang, X. Miao, C. Wang, C. Wang, Z. Zhang, R. Wang, L. Yin, *Batteries Supercaps* **2022**, 5, e202100288.
- [62] C. Zheng, L. Li, K. Wang, C. Wang, J. Zhang, Y. Xia, H. Huang, C. Liang, Y. Gan, X. He, X. Tao, W. Zhang, *Batteries Supercaps* **2021**, 4, 8.
- [63] L. Hu, X. Gao, H. Wang, Y. Song, Y. Zhu, Z. Tao, B. Yuan, R. Hu, *Small* **2024**, 20, 2312251.
- [64] W. Yang, W. Yang, J. Zeng, Y. Chen, Y. Huang, J. Liu, J. Gan, T. Li, H. Zhang, L. Zhong, X. Peng, *Prog. Mater. Sci.* **2024**, 144, 101264.

- [65] L. Zhou, D. L. Danilov, R. Eichel, P. H. L. Notten, *Adv. Energy Mater.* **2021**, *11*, 2001304.
- [66] S. Feng, Z. Fu, X. Chen, Q. Zhang, *InfoMat* **2022**, *4*, e12304.
- [67] X. Li, Z. Chu, H. Jiang, Y. Dai, W. Zheng, A. Liu, X. Jiang, G. He, *Energy Storage Mater.* **2021**, *37*, 233.
- [68] J. Chen, H. Zhang, M. Fang, C. Ke, S. Liu, J. Wang, *ACS Energy Lett.* **2023**, *8*, 1723.
- [69] T. Sun, Q. Nian, X. Ren, Z. Tao, *Joule* **2023**, *7*, 2700.
- [70] Q. Lin, D. Kundu, M. Skyllas-Kazacos, J. Lu, D. Zhao, K. Amine, L. Dai, D. Wang, *Adv. Mater.* **2024**, *36*, 2406151.
- [71] D. Li, Y. Ouyang, H. Lu, Y. Xie, S. Guo, Q. Zeng, Y. Xiao, Q. Zhang, S. Huang, *Mater. Today Chem.* **2023**, *32*, 101629.
- [72] Y. Zhao, L. Li, Y. Shan, D. Zhou, X. Chen, W. Cui, H. Wang, *Small* **2023**, *19*, 2301572.
- [73] P. Chang, Z. Liu, M. Xi, Y. Guo, T. Wu, J. Ding, H. Liu, Y. Huang, *Adv. Powder Mater.* **2025**, *4*, 100263.
- [74] H. An, M. Li, Q. Liu, Y. Song, J. Liu, Z. Yu, X. Liu, B. Deng, J. Wang, *Nat. Commun.* **2024**, *15*, 9150.
- [75] L. Fu, S. Zhou, M. Xiang, J. Yang, W. Fan, Z. Yang, J. Ou, *J. Electroanal. Chem.* **2022**, *921*, 116650.
- [76] J. Tang, X. Liu, X. Wang, J. Chi, Z. Xiao, Z. Wu, L. Wang, *Inorg. Chem. Front.* **2024**, *11*, 5384.
- [77] R. Wei, Y. Lu, Y. Xu, *Sci. China Chem.* **2021**, *64*, 1826.
- [78] Z. Kong, M. Huang, Z. Liang, H. Tu, K. Zhang, Y. Shao, Y. Wu, X. Hao, *Inorg. Chem. Front.* **2022**, *9*, 902.
- [79] H. Liu, Y. Ye, F. Zhu, X. Zhong, D. Luo, Y. Zhang, W. Deng, G. Zou, H. Hou, X. Ji, *Angew. Chem. Int. Ed.* **2024**, *63*, e202409044.
- [80] Y. Zhao, L. Li, D. Zhou, Y. Ma, Y. Zhang, H. Yang, S. Fan, H. Tong, S. Li, W. Qu, *Angew. Chem. Int. Ed.* **2024**, *63*, e202404728.
- [81] B. Luo, W. Wang, Q. Wang, W. Ji, G. Yu, Z. Liu, Z. Zhao, X. Wang, S. Wang, J. Zhang, *Chem. Eng. J.* **2023**, *460*, 141329.
- [82] H. Wang, C. Lei, T. Liu, C. Xu, X. He, X. Liang, *Angew. Chem. Int. Ed.* **2024**, *63*, e202401483.
- [83] M. Li, X. Wang, J. Meng, C. Zuo, B. Wu, C. Li, W. Sun, L. Mai, *Adv. Mater.* **2024**, *36*, 2308628.
- [84] Z. Su, J. Chen, J. Stansby, C. Jia, T. Zhao, J. Tang, Y. Fang, A. Rawal, J. Ho, C. Zhao, *Small* **2022**, *18*, 2201449.
- [85] L. Sieuw, A. Jouhara, É. Quarez, C. Auger, J. F. Gohy, P. Poizot, A. Vlad, *Chem. Sci.* **2019**, *10*, 418.
- [86] Y. Wang, L. Wu, Z. Lin, M. Tang, P. Ding, X. Guo, Z. Zhang, S. Liu, B. Wang, X. Yin, Z. Chen, K. Amine, H. Yu, *Nano Energy* **2022**, *96*, 107105.
- [87] G. Chen, Y. Zhang, C. Zhang, W. Ye, J. Wang, Z. Xue, *ChemSusChem* **2022**, *15*, e202201361.
- [88] C. Ling, T. Naren, X. Liu, J. Yang, P. Xiao, W. Wei, X. Ji, G. C. Kuang, L. Chen, *Mater. Today Energy* **2023**, *36*, 101372.
- [89] X. Lin, S. Xu, Y. Tong, X. Liu, Z. Liu, P. Li, R. Liu, X. Feng, L. Shi, Y. Ma, *Mater. Horiz.* **2023**, *10*, 859.
- [90] Z. Lv, Y. Tang, S. Dong, Q. Zhou, G. Cui, *Chem. Eng. J.* **2022**, *430*, 132659.
- [91] Y. Ye, X. Zhu, N. Meng, F. Lian, *Adv. Funct. Mater.* **2023**, *33*, 2307045.
- [92] H. Xu, W. Deng, L. Shi, J. Long, Y. Zhang, L. Xu, L. Mai, *Angew. Chem. Int. Ed.* **2024**, *63*, e202400032.
- [93] K. Hashimoto, T. Shiwaku, H. Aoki, H. Yokoyama, K. Mayumi, K. Ito, *Sci. Adv.* **2023**, *9*, eadi8505.
- [94] Z. Shi, J. Wang, K. Guo, H. Wang, H. Nie, Z. Xue, *Chem. Eng. J.* **2023**, *468*, 143687.
- [95] H. Zhang, L. Li, G. Kang, N. Lu, S. Wang, G. Wang, *ACS Appl. Mater. Interfaces* **2024**, *16*, 24671.
- [96] A. J. Butzelaar, P. Röring, M. Hoffmann, J. Atik, E. Paillard, M. Wilhelm, M. Winter, G. Brunklaus, P. Theato, *Macromolecules* **2021**, *54*, 11101.
- [97] J. Han, M. J. Lee, J. H. Min, K. H. Kim, K. Lee, S. H. Kwon, J. Park, K. Ryu, H. Seong, H. Kang, E. Lee, S. W. Lee, B. J. Kim, *Adv. Funct. Mater.* **2024**, *34*, 2310801.
- [98] W. Ma, X. Cui, Y. Chen, S. Wan, S. Zhao, J. Gong, G. Wang, S. Chen, *Angew. Chem. Int. Edit.* **2025**, *64*, e202415617.
- [99] L. Li, Y. Shan, F. Wang, X. Chen, Y. Zhao, D. Zhou, H. Wang, W. Cui, *ACS Appl. Mater. Interfaces* **2021**, *13*, 48525.
- [100] H. Peng, T. Long, J. Peng, H. Chen, L. Ji, H. Sun, L. Huang, S. Sun, *Adv. Energy Mater.* **2024**, *14*, 2400428.
- [101] Q. Zeng, P. Chen, Z. Li, X. Wen, W. Wen, Y. Liu, H. Zhao, S. Zhang, H. Zhou, L. Zhang, *ACS Appl. Mater. Interfaces* **2021**, *13*, 48569.
- [102] Y. Liang, N. Chen, W. Qu, C. Yang, L. Li, F. Wu, R. Chen, *ACS Appl. Mater. Interfaces* **2021**, *13*, 42957.
- [103] Y. Wang, H. Tu, A. Sun, L. Wang, F. Zhu, P. Xue, J. Wang, F. Ye, M. Liu, *Chem. Eng. J.* **2023**, *475*, 146414.
- [104] G. Feng, Q. Ma, D. Luo, T. Yang, Y. Nie, Z. Zheng, L. Yang, S. Li, Q. Li, M. Jin, X. Wang, Z. Chen, *Angew. Chem. Int. Edit.* **2025**, *64*, e202413306.
- [105] X. Zhao, Z. Fu, X. Zhang, X. Wang, B. Li, D. Zhou, F. Kang, *Energy Environ. Sci.* **2024**, *17*, 2406.
- [106] J. Xu, *Mater. Futur.* **2023**, *2*, 047501.
- [107] R. Kang, D. Zhang, Y. Du, C. Sun, W. Zhou, H. Wang, J. Wan, G. Chen, J. Zhang, *Small* **2024**, *20*, 2305998.
- [108] Y. Chen, H. Fu, Y. Huang, L. Huang, X. Zheng, Y. Dai, Y. Huang, W. Luo, *ACS Mater. Lett.* **2021**, *3*, 160.
- [109] X. Zhou, W. B. Zhang, X. W. Han, S. S. Chai, S. B. Guo, X. L. Zhang, L. Zhang, X. Bao, Y. W. Guo, X. J. Ma, *ACS Appl. Energy Mater.* **2022**, *5*, 3979.
- [110] B. Ouyang, Y. Zeng, *Nat. Commun.* **2024**, *15*, 973.
- [111] Z. Zhou, Y. Ma, T. Brezesinski, B. Breitung, Y. Wu, Y. Ma, *Energy Environ. Sci.* **2025**, *18*, 19.
- [112] Y. Yao, Q. Dong, A. Brozena, J. Luo, J. Miao, M. Chi, C. Wang, I. G. Kevrekidis, Z. J. Ren, J. Greeley, G. Wang, A. Anapolsky, L. Hu, *Science* **2022**, *376*, eabn3103.
- [113] J. Tian, Y. Rao, W. Shi, J. Yang, W. Ning, H. Li, Y. Yao, H. Zhou, S. Guo, *Angew. Chem. Int. Edit.* **2023**, *62*, e202310894.
- [114] Z. Wang, H. Ge, S. Liu, G. Li, X. Gao, *Energy Environ. Mater.* **2023**, *6*, e12358.
- [115] R. He, L. Yang, Y. Zhang, X. Wang, S. Lee, T. Zhang, L. Li, Z. Liang, J. Chen, J. Li, A. Ostovari Moghaddam, J. Llorca, M. Ibáñez, J. Arbiol, Y. Xu, A. Cabot, *Energy Storage Mater.* **2023**, *58*, 287.
- [116] Y. Su, X. Rong, H. Li, X. Huang, L. Chen, B. Liu, Y. Hu, *Adv. Mater.* **2023**, *35*, 2209402.
- [117] G. Ye, L. Zhu, Y. Ma, M. He, C. Zheng, K. Shen, X. Hong, Z. Xiao, Y. Jia, P. Gao, Q. Pang, *J. Am. Chem. Soc.* **2024**, *146*, 27668.
- [118] H. Zhang, Y. Wang, J. Huang, W. Li, X. Zeng, A. Jia, H. Peng, X. Zhang, W. Yang, *Energy Environ. Mater.* **2024**, *7*, e12514.
- [119] X. Ma, Y. Lu, Y. Ou, S. Yan, W. Hou, P. Zhou, K. Liu, *Nano Res.* **2024**, *17*, 8754.
- [120] X. Liu, H. Jia, H. Li, *Energy Storage Mater.* **2024**, *67*, 103263.
- [121] X. Zhu, Z. Wang, Z. Fang, Z. Xu, B. Luo, H. Yang, K. Wang, B. Guo, *J. Energy Storage* **2025**, *108*, 115080.
- [122] J. L. Olmedo-Martínez, L. Meabe, R. Riva, G. Guzmán-González, L. Porcarelli, M. Forsyth, A. Mugica, I. Calafel, A. J. Müller, P. Lecomte, C. Jérôme, D. Mecerreyres, *Polym. Chem.* **2021**, *12*, 3441.
- [123] J. Xiang, Y. Zhang, B. Zhang, L. Yuan, X. Liu, Z. Cheng, Y. Yang, X. Zhang, Z. Li, Y. Shen, J. Jiang, Y. Huang, *Energy Environ. Sci.* **2021**, *14*, 3510.
- [124] M. Wu, S. Han, S. Liu, J. Zhao, W. Xie, *Energy Storage Mater.* **2024**, *66*, 103174.
- [125] K. Deng, T. Guan, F. Liang, X. Zheng, Q. Zeng, Z. Liu, G. Wang, Z. Qiu, Y. Zhang, M. Xiao, Y. Meng, L. Wei, *J. Mater. Chem. A* **2021**, *9*, 7692.
- [126] Y. Liao, X. Xu, X. Luo, S. Ji, J. Zhao, J. Liu, Y. Huo, *Batteries* **2023**, *9*, 439.
- [127] J. Jeong, M. Kim, H. Shin, H. Lee, Y. G. Cho, M. Cho, J. Lee, C. Han, G. Kim, H. Lee, H. Lee, T. H. Kim, S. H. Jung, H.-K. Song, *ACS Energy Lett.* **2023**, *8*, 4650.
- [128] B. Zhou, C. Yang, F. Wu, T. Deng, S. Guo, G. Zhu, Y. Jiang, Z. Wang, *Chem. Eng. J.* **2022**, *450*, 138385.
- [129] H. J. Cheon, T. T. Vu, M. Woo, Y. Kim, H. Choi, J. Kim, Y. Choi, Y. A. Kim, J. W. Yun, Y. Ko, M. Chang, *ACS Sustain. Chem. Eng.* **2024**, *12*, 2686.
- [130] Z. Li, S. Zhu, S. Gao, Y. He, H. Ding, D. Yang, H. Yang, P. Cao, *Adv. Funct. Mater.* **2024**, *34*, 2409836.
- [131] Z. Zhang, T. Zhao, S. Huang, S. Wang, D. Han, H. Guo, M. Xiao, Y. Meng, *Adv. Energy Mater.* **2024**, *15*, 2403678.
- [132] F. Pei, L. Wu, Y. Zhang, Y. Liao, Q. Kang, Y. Han, H. Zhang, Y. Shen, H. Xu, Z. Li, Y. Huang, *Nat. Commun.* **2024**, *15*, 351.
- [133] H. Zhang, X. Xu, W. Fan, J. Zhao, Y. Huo, *Chem. – Eur. J.* **2024**, *30*, e202402798.
- [134] Y. Liu, J. Cai, W. Chang, Y. Tan, C. Lai, Y. Peng, H. Liu, *ACS Appl. Energy Mater.* **2024**, *7*, 4303.
- [135] Z. Rong, Y. Xu, J. Wang, R. Liu, F. Cheng, W. Zhang, *J. Power Sources* **2025**, *630*, 236151.
- [136] H. Zhang, J. Deng, H. Xu, H. Xu, Z. Xiao, F. Fei, W. Peng, L. Xu, Y. Cheng, Q. Liu, G. Hu, L. Mai, *Adv. Mater.* **2024**, *36*, 2403848.
- [137] Y. Zhu, Z. Lao, M. Zhang, T. Hou, X. Xiao, Z. Piao, G. Lu, Z. Han, R. Gao, L. Nie, X. Wu, Y. Song, C. Ji, J. Wang, G. Zhou, *Nat. Commun.* **2024**, *15*, 3914.
- [138] J. Suo, Q. Zhao, H. Tian, L. Wang, L. Dai, J. Luo, S. Liu, *ACS Nano* **2023**, *17*, 10229.
- [139] Y. Zhao, L. Li, H. Yang, S. Fan, S. Li, H. Tong, *Energy Storage Mater.* **2024**, *65*, 103126.

- [140] Y. Zhao, L. Li, D. Zhou, H. Yang, S. Fan, S. Li, H. Tong, W. Qu, *Adv. Funct. Mater.* **2024**, *34*, 2408379.
- [141] H. Wan, J. Xu, C. Wang, *Nat. Rev. Chem.* **2023**, *8*, 30.
- [142] J. Xiao, N. Adelstein, Y. Bi, W. Bian, J. Cabana, C. L. Cobb, Y. Cui, S. J. Dillon, M. M. Doeff, S. M. Islam, K. Leung, M. Li, F. Lin, J. Liu, H. Luo, A. C. Marschilok, Y. S. Meng, Y. Qi, R. Sahore, K. G. Sprenger, R. C. Tenent, M. F. Toney, W. Tong, L. F. Wan, C. Wang, S. E. Weitzner, B. Wu, Y. Xu, *Nat. Energy* **2024**, *9*, 1463.
- [143] J. W. Choi, D. Aurbach, *Nat. Rev. Mater.* **2016**, *1*, 16013.
- [144] H. Adenusi, G. A. Chass, S. Passerini, K. V. Tian, G. Chen, *Adv. Energy Mater.* **2023**, *13*, 2203307.
- [145] K. Z. Walle, Y. S. Wu, W. C. Chien, M. Kotobuki, S. H. Wu, C. C. Yang, *J. Mater. Chem. A* **2024**, *12*, 14099.
- [146] J. Ling, C. Karuppiyah, I. I. Misnon, H. J. Lee, C. C. Yang, R. Jose, *Energy Fuels* **2024**, *38*, 18292.
- [147] M. M. Jia, J. H. Feng, W. Shao, Z. Chen, J. R. Yu, J. J. Sun, Q. Y. Wu, Y. Li, M. Xue, X. M. Chen, *J. Membr. Sci.* **2024**, *694*, 122418.
- [148] X. Kong, X. Zong, Z. Lei, Z. Wang, Y. Zhao, X. Zhao, J. Zhang, Z. Liu, Y. Ren, L. Wu, M. Zhang, F. He, P. Yang, *Small* **2024**, *20*, 2405174.
- [149] K. Li, J. Wang, Q. Shen, Y. Song, R. Gao, Y. Wang, *Adv. Energy Mater.* **2024**, *14*, 2400956.
- [150] L. Ma, J. Tan, Z. Ren, B. Feng, Z. Liu, P. Yi, S. Cao, W. Lu, Y. Liu, C. Ye, M. Ye, H. Fang, J. Shen, *Adv. Funct. Mater.* **2025**, *35*, 2414816.

Manuscript received: February 20, 2025

Revised manuscript received: April 30, 2025

Version of record online: May 9, 2025